

1 **Export fluxes in a naturally iron-fertilized area of the Southern**  
2 **Ocean: seasonal dynamics of particulate organic carbon export**  
3 **from a moored sediment trap (part 1).**

4  
5 M. Rembauville<sup>1,2</sup>, I. Salter<sup>1,2,3</sup>, N. Leblond<sup>4,5</sup>, A. Gueneugues<sup>1,2</sup> and S. Blain<sup>1,2</sup>

6 <sup>1</sup> Sorbonne Universités, UPMC Univ Paris 06, UMR 7621, LOMIC, Observatoire Océanologique, Banyuls-sur-Mer, France.

7  
8 <sup>2</sup> CNRS, UMR 7621, LOMIC, Observatoire Océanologique, Banyuls-sur-Mer, France.

9  
10 <sup>3</sup> Alfred-Wegener-Institute for Polar and Marine research, Bremerhaven, Germany.

11  
12 <sup>4</sup> Sorbonne Universités, UPMC Univ Paris 06, LOV, UMR 7093, Observatoire Océanologique, Villefranche-sur-Mer, France

13  
14 <sup>5</sup> CNRS-INSU, LOV, UMR 7093, Observatoire Océanologique, Villefranche-sur-Mer, France

15  
16  
17 Correspondance to: M. Rembauville ([rembauville@obs-banyuls.fr](mailto:rembauville@obs-banyuls.fr)).

18  
19  
20 **Abstract**

21  
22 A sediment trap moored in the naturally iron-fertilized Kerguelen plateau in the Southern  
23 Ocean provided an annual record of particulate organic carbon and nitrogen fluxes at 289 m.  
24 At the trap deployment depth current speeds were typically low ( $\sim 10 \text{ cm s}^{-1}$ ) and primarily  
25 tidal-driven (M2 tidal component). Although advection was weak, the sediment trap may have  
26 been subject to hydrodynamical and biological (swimmer feeding on trap funnel) biases.  
27 Particulate organic carbon (POC) flux was generally low ( $< 0.5 \text{ mmol m}^{-2} \text{ d}^{-1}$ ) although two  
28 episodic export events ( $< 14$  days) of  $1.5 \text{ mmol m}^{-2} \text{ d}^{-1}$  were recorded. These increases in flux  
29 occurred with a 1-month time lag from peaks in surface chlorophyll and together accounted  
30 for approximately 40 % of the annual flux budget. The annual POC flux of  $98.2 \pm 4.4 \text{ mmol m}^{-2}$   
31  $\text{y}^{-1}$  was low considering the shallow deployment depth, but comparable to independent

32 estimates made at similar depths (~300 m) over the plateau and to deep-ocean (>2 km) fluxes  
33 measured from similarly productive iron-fertilized blooms. Although undertrapping cannot be  
34 excluded in shallow moored sediment trap deployment, we hypothesize that grazing pressure,  
35 including mesozooplankton and mesopelagic fishes, may be responsible for the significant  
36 reduction in POC flux beneath the base of the winter mixed layer. The importance of plankton  
37 community structure in controlling the temporal variability of export fluxes is addressed in a  
38 companion paper.

39

## 40 **1 Introduction**

41           The biological carbon pump is defined as the vertical transfer of biologically fixed  
42 carbon in the ocean surface to the ocean interior (Volk and Hoffert, 1985). Global estimates of  
43 Particulate Organic Carbon (POC) export cluster between  $5 \text{ Pg C y}^{-1}$  (Moore et al., 2004; Lutz  
44 et al., 2007; Honjo et al., 2008; Henson et al., 2011; Lima et al., 2014) to  $10 \text{ Pg C y}^{-1}$  (Laws et  
45 al., 2000; Schlitzer, 2004; Gehlen et al., 2006; Boyd and Trull, 2007; Dunne et al., 2007;  
46 Laws et al., 2011). The physical transfer of dissolved inorganic carbon to the ocean interior  
47 during subduction of water masses is two orders of magnitude higher ( $> 250 \text{ Pg C y}^{-1}$ ,  
48 Karleskind et al., 2011; Levy et al., 2013). The global ocean represents a net annual  $\text{CO}_2$  sink  
49 of  $2.5 \text{ Pg C y}^{-1}$  (Le Quéré et al., 2013), slowing down the increase of the atmospheric  $\text{CO}_2$   
50 concentration resulting from anthropogenic activity. Although the Southern Ocean (south of  
51  $44^\circ\text{S}$ ) plays a limited role in the net air-sea  $\text{CO}_2$  flux (Lenton et al., 2013), it is a key  
52 component of the global anthropogenic  $\text{CO}_2$  sink representing one third the global oceanic  
53 sink ( $\sim 1 \text{ Pg C y}^{-1}$ ) while covering 20 % of its surface (Gruber et al., 2009). The solubility  
54 pump is considered as the major component of this sink, whereas the biological carbon pump  
55 is considered to be inefficient in the Southern Ocean and sensitive to iron supply.

56           Following “the iron hypothesis” in the nineties (Martin 1990), iron limitation of high  
57 nutrient low chlorophyll (HNLC) areas, including the Southern Ocean, has been tested in  
58 bottle experiments (de Baar et al., 1990) and through *in situ* artificial fertilization experiments  
59 (de Baar et al., 2005; Boyd et al., 2007). Results from these experiments are numerous and  
60 essentially highlight that iron limits macronutrient (N, P, Si) utilization (Boyd et al., 2005;  
61 Hiscock and Millero, 2005) and primary production (Landry et al., 2000; Gall et al., 2001;  
62 Coale et al., 2004) in these vast HNLC areas of the Southern Ocean. Due to a large  
63 macronutrient repository the biological carbon pump in the Southern Ocean is considered to  
64 be inefficient in its capacity to transfer atmospheric carbon to the ocean interior (Sarmiento

65 and Gruber, 2006). In the context of micronutrient limitation, sites enriched in iron by natural  
66 processes have also been studied and include the Kerguelen islands (Blain et al., 2001, 2007),  
67 the Crozet islands (Pollard et al., 2007), the Scotia Sea (Tarling et al., 2012), and the Drake  
68 Passage (Measures et al., 2013). Enhanced primary producer biomass in association with  
69 natural iron supply (Korb and Whitehouse, 2004; Seeyave et al., 2007; Lefèvre et al., 2008)  
70 strongly support trace-metal limitation. Furthermore, indirect seasonal budgets constructed  
71 from studies of naturally fertilized systems have been capable of demonstrating an increase in  
72 the strength of the biological carbon pump (Blain et al., 2007; Pollard et al., 2009), although  
73 strong discrepancies in carbon to iron sequestration efficiency exist between systems. To date,  
74 direct measurements of POC export from naturally fertilized blooms in the Southern Ocean  
75 are limited to the Crozet Plateau (Pollard et al., 2009; Salter et al., 2012). The HNLC  
76 Southern Ocean represents a region where changes in the strength of the biological pump may  
77 have played a role in the glacial-interglacial CO<sub>2</sub> cycles (Bopp et al., 2003; Kohfeld et al.,  
78 2005) and have some significance to future anthropogenic CO<sub>2</sub> uptake (Sarmiento and Le  
79 Quéré, 1996). In this context, additional studies that directly measure POC export from  
80 naturally iron-fertilized blooms in the Southern Ocean are necessary.

81 POC export can be estimated at short timescales (days to weeks) using the <sup>234</sup>Th proxy  
82 (Coale and Bruland, 1985; Buesseler et al., 2006; Savoye et al., 2006), by optical imaging of  
83 particles (e.g. Picheral et al., 2010) or by directly collecting particles into surface-tethered  
84 sediment traps (e.g. Maiti et al., 2013 for a compilation in the Southern Ocean) or neutrally  
85 buoyant sediment traps (e.g. Salter et al., 2007; Rynearson et al., 2013). Temporal variability  
86 of flux in the Southern Ocean precludes extrapolation of discrete measurements to estimate  
87 seasonal or annual carbon export. However seasonal export of POC can be derived from  
88 biogeochemical budgets (Blain et al., 2007; Pollard et al., 2009) or be directly measured by  
89 moored sediment traps (e.g. Salter et al., 2012). Biogeochemical budgets are capable of

90 integrating over large spatial and temporal scales but may incorporate certain assumptions and  
91 lack information about underlying mechanisms. Direct measurement by sediment traps rely  
92 on fewer assumptions but their performance is strongly related to prevailing hydrodynamic  
93 conditions (Buesseler et al., 2007a), which can be particularly problematic in the surface  
94 ocean. Measuring the hydrological conditions characterizing mooring deployments is  
95 therefore crucial to address issues surrounding the efficiency of sediment trap collection.

96         The ecological processes responsible for carbon export remain poorly characterized  
97 (Boyd and Trull, 2007). There is a strong requirement for quantitative analysis of the  
98 biological components of export to elucidate patterns in carbon and biomineral fluxes to the  
99 ocean interior (Francois et al., 2002; Salter et al., 2010; Henson et al., 2012; Le Moigne et al.,  
100 2012; Lima et al., 2014). Long-term deployment of moored sediment traps in areas of  
101 naturally iron fertilized production, where significant macro- and micro-nutrient gradients  
102 seasonally structure plankton communities, can help to establish links between ecological  
103 succession and carbon export. For example, sediment traps around the Crozet Plateau (Pollard  
104 et al., 2009) identified the significance of *Eucampia antarctica* var. *antarctica* resting spores  
105 for carbon transfer to the deep ocean, large empty diatom frustules for Si:C export  
106 stoichiometry (Salter et al., 2012), and heterotrophic calcifiers for the carbonate counter pump  
107 (Salter et al., 2014).

108         The increase in primary production resulting from natural fertilization might not  
109 necessarily lead to significant increases in carbon export. The concept of “High Biomass, Low  
110 Export” (HBLE) environments was first introduced in the Southern Ocean (Lam and Bishop,  
111 2007). This concept is partly based on the idea that a strong grazer response to phytoplankton  
112 biomass leads to major fragmentation and remineralization of particles in the twilight zone,  
113 shallowing the remineralization horizon (Coale et al., 2004). In these environments, the  
114 efficient utilization and reprocessing of exported carbon by zooplankton leads to fecal pellet

115 dominated, low POC fluxes (Ebersbach et al., 2011). A synthesis of short-term sediment trap  
116 deployments, <sup>234</sup>Th estimates of upper ocean POC export and in situ primary production  
117 measurements in the Southern Ocean by Maiti et al. (2013) has highlighted the inverse  
118 relationship between primary production and export efficiency, verifying the HBLE status of  
119 many productive areas in the Southern Ocean. The iron fertilized bloom above the Kerguelen  
120 Plateau exhibits strong remineralization in the mixed layer compared to the mesopelagic,  
121 (Jacquet et al., 2008) and high bacterial carbon demand (Obernosterer et al., 2008), features  
122 consistent with a HBLE regime. Moreover, an inverse relationship between export efficiency  
123 and zooplankton biomass in the Kerguelen Plateau region support the key role of grazers in  
124 the HBLE scenario (Laurenceau-Cornec et al., 2015). Efficient grazer responses to  
125 phytoplankton biomass following artificial iron fertilization of HNLC regions also  
126 demonstrate increases in net community production that are not translated to an increase in  
127 export fluxes (Lam and Bishop, 2007; Tsuda et al., 2007; Martin et al., 2013; Batten and  
128 Gower, 2014).

129 POC flux attenuation with depth results from processes occurring in the euphotic layer  
130 (setting the particle export efficiency, Henson et al., 2012) and processes occurring in the  
131 twilight zone between the euphotic layer and ~1000 m (Buesseler and Boyd, 2009), setting  
132 the transfer efficiency (Francois et al., 2002). These processes are mainly biologically-driven  
133 (Boyd and Trull, 2007) and involve a large diversity of ecosystem components from bacteria  
134 (Rivkin and Legendre, 2001; Giering et al., 2014), protozooplankton (Barbeau et al., 1996),  
135 mesozooplankton (Dilling and Alldredge, 2000; Smetacek et al., 2004) and mesopelagic  
136 fishes (Davison et al., 2013; Hudson et al., 2014). The net effect of these processes is  
137 summarized in a power-law formulation of POC flux attenuation with depth proposed by  
138 Martin et al. (1987) that is still commonly used in data and model applications. The b-  
139 exponent in this formulation has been reported to range from 0.4 to 1.7 (Buesseler et al.,

140 2007b; Lampitt et al., 2008; Henson et al., 2012) in the global Ocean. Nevertheless, a change  
141 in the upper mesopelagic community structure (Lam et al., 2011), and more precisely an  
142 increasing contribution of mesozooplankton (Lam and Bishop, 2007; Ebersbach et al., 2011)  
143 could lead to a shift toward higher POC flux attenuation with depth.

144         In this paper, we provide the first annual description of the POC and PON export  
145 fluxes below the mixed layer within the naturally fertilized bloom of the Kerguelen Plateau  
146 and we discuss the reliability of these measurements considering the hydrological and  
147 biological context. A companion paper (Rembauville et al., 2014) addresses our final aim: to  
148 identify the ecological vectors that explain the intensity and the stoichiometry of the fluxes.

## 149 2 Material and Methods

### 150 2.1 Trap deployment and mooring design

151 As part of the KEOPS2 multidisciplinary program, a mooring line was deployed at  
152 station A3 (50°38.3 S – 72°02.6 E) in the Permanently Open Ocean Zone (POOZ), south of  
153 the Polar Front (PF) (Fig. 1). The mooring line was instrumented with a Technicap PPS3  
154 (0.125 m<sup>2</sup> collecting area, 4.75 aspect ratio) sediment trap and inclinometer (NKE S2IP) at a  
155 depth of 289 m (seafloor depth 527 m) (Fig. 2). A conductivity-temperature-pressure (CTD)  
156 sensor (Seabird SBE 37) and a current meter (Nortek Aquadopp) were placed on the mooring  
157 line 30 m beneath the sediment trap (319 m). The sediment trap collection period started on  
158 21 October 2011 until 7 September 2012. The sediment trap was composed of twelve rotating  
159 sample cups (250 mL) filled with a 5 % formalin hypersaline solution buffered with sodium  
160 tetraborate at pH = 8. Rotation of the carousel was programmed to sample short intervals (10-  
161 14 days) between October and February, to optimize the temporal resolution of export from  
162 the bloom, and long intervals (99 days) between February and September. All instruments had  
163 a 1 hour recording interval. The current meter failed on the 7<sup>th</sup> April 2012.

### 164 2.3 Surface chlorophyll data

165 The MODIS AQUA level 3 (4 km grid resolution, 8 day averages) surface chlorophyll  
166 *a* product was extracted from the NASA website (<http://oceancolor.gsfc.nasa.gov/>) for  
167 sediment trap deployment period. An annual climatology of surface chlorophyll *a*  
168 concentration, based on available satellite products (1997-2013), was calculated from the  
169 multisatellite Globcolour product. The Globcolour level 3, (case 1 waters, 4.63 km resolution,  
170 8 day averages) product merging Seawifs, MODIS and MERIS data with GSM merging  
171 model (Maritorena and Siegel, 2005) was accessed via <http://www.globcolour.info>. Surface  
172 chlorophyll *a* concentrations derived from Globcolour (climatology) and MODIS data



173 (deployment year) were averaged across a 100 km radius centered on the sediment trap  
174 deployment location (Fig. 1).

### 175 **2.3 Time series analyses of hydrological parameters**

176 Fast Fourier Transform (FFT) analysis was performed on the annual time series data obtained  
177 from the mooring, depth and potential density anomaly ( $\sigma_\theta$ ) that were derived from the CTD  
178 sensor. Significant peaks in the power spectrum were identified by comparison to red noise, a  
179 theoretical signal in which the relative variance decreases with increasing frequency (Gilman  
180 et al., 1963). The red noise signal was considered as a null hypothesis and its power spectrum  
181 was scaled to the 99<sup>th</sup> percentile of  $\chi^2$  probability. Power peaks higher than 99 % red noise  
182 values were considered to be statistically significant (Schulz and Mudelsee, 2002), enabling  
183 the identification of periods of major variability in time series. In order to identify the water  
184 masses surrounding the trap, temperature and salinity recorded by the mooring CTD were  
185 placed in context to previous CTD casts conducted at A3 during KEOPS1 (39 profiles, 23  
186 January 2005 - 13 February 2005) and KEOPS2 (12 profiles, from 15 - 17 November).

### 187 **2.4 Sediment trap material analyses**

188 Upon recovery of the sediment trap the pH of the supernatant was measured in every cup and  
189 1 mL of 37 % formalin buffered with sodium tetraborate (pH=8) was added. After allowing  
190 the particulate material to settle to the base of the sample cup (~24 hrs), 60 mL of supernatant  
191 was removed with a syringe and stored separately. The samples were transported in the dark  
192 at 4°C (JGOFS Sediment Trap Methods, 1994) and stored under identical conditions upon  
193 arrival at the laboratory until further analysis. Nitrate, nitrite, ammonium and phosphate in the  
194 supernatant were analysed colorimetrically (Aminot and Kerouel, 2007) to check for possible  
195 leaching of dissolved inorganic nitrogen and phosphorus from the particulate phase.

196 Samples were first transferred to a petri dish and examined under stereomicroscope  
197 (Leica MZ8, x10 to x50 magnification) to determine and isolate swimmers (i.e. organisms  
198 that actively entered the cup). All swimmers were carefully sorted, cleaned (rinsed with  
199 preservative solution), enumerated and removed from the cups for further taxonomic  
200 identification. The classification of organisms as swimmers remains subjective and there is no  
201 standardized protocol. We classified zooplankton organisms as swimmers if organic material  
202 and preserved structures could be observed. Empty shells, exuvia (exoskeleton remains) and  
203 organic debris were considered part of the passive flux. Sample preservation prevented the  
204 identification of smaller swimmers (mainly copepods) but, where possible, zooplankton were  
205 identified following Boltovskoy (1999).

206 Following the removal of swimmers, samples were quantitatively split into eight  
207 aliquots using a Jencons peristaltic splitter. A splitting precision of 2.9 % (coefficient of  
208 variation) was determined by weighing the particulate material obtained from each of four  
209 1/8<sup>th</sup> aliquots (see below). Aliquots for chemical analyses were centrifuged (5 min at 3000  
210 rpm) with the supernatant being withdrawn after this step and replaced by milliQ-grade water  
211 to remove salts. Milli-Q rinses were compared with ammonium formate. Organic carbon  
212 content was not statistically different although nitrogen concentrations were significantly  
213 higher, consequently Milli-Q rinses were routinely performed. The rinsing step was repeated  
214 three times. The remaining pellet was freeze-dried (SGD-SERAIL, 0.05-0.1 mbar, -30 °C to  
215 30 °C, 48h run) and weighed three times (Sartorius MC 210 P balance, precision 10<sup>-4</sup> g) to  
216 calculate the total mass. The particulate material was ground to a fine powder and used for  
217 measurements of particulate constituents.

218 For particulate organic carbon (POC) and particulate organic nitrogen (PON) analyses,  
219 3 to 5 mg of the freeze-dried powder was weighed directly into pre-combusted (450°C, 24h)  
220 silver cups. Samples were decarbonated by adding 20 µL of 2M analytical grade Hydrochloric

221 acid (Sigma-Aldrich). Acidification was repeated until no bubbles could be seen, ensuring all  
222 particulate carbonate was dissolved (Salter et al., 2010). Samples were dried overnight at 50  
223 °C. POC and PON were measured with a CHN analyzer (Perkin Elmer 2400 Series II  
224 CHNS/O Elemental Analyzer) calibrated with glycine. Samples were analysed in triplicate  
225 with an analytical precision of less than 0.7 %. Due to the small amount of particulate  
226 material in sample cups #5 and #12, replicate analyses were not possible. Uncertainty  
227 propagation for POC and PON flux was calculated as the quadratic sum of errors on mass flux  
228 and POC/PON content in each sample. The annual flux ( $\pm$  standard deviation) was calculated  
229 as the sum of the time-integrated flux.

### 230 **3. Results**

#### 231 **3.1 Physical conditions around trap**

232 The sediment trap was deployed in the upper layers of Upper Circumpolar Deep Water  
233 (UCDW), beneath seasonally mixed Winter Water (WW) (Fig. 2). The depth of the CTD  
234 sensor varied between 318 m and 322 m (1 % and 99 % quantiles), with rare deepening to 328  
235 m (Fig. 3a). Variations in tilt angle of the sediment trap were also low, mostly between 1 °  
236 and 5 °, and occasionally reaching 13 ° (Fig. 3d). Current speed amplitude varied between 4  
237  $\text{cm s}^{-1}$  and 23  $\text{cm s}^{-1}$  (1 % and 99 % quantiles) with a maximum value of 33  $\text{cm s}^{-1}$  and a mean  
238 value of 9  $\text{cm s}^{-1}$  (Fig. 3e). Horizontal flow vectors were divided between northward and  
239 southward components with strongest current speeds observed to flow northward (Fig. 3f and  
240 3g).

241 The range in potential temperature and salinity was 1.85–2.23 °C and 34.12 – 34.26 (1  
242 % - 99 % quantiles) (Fig. 3b and 3c). From July to September 2012, a mean increase of 0.2°C  
243 in potential temperature was associated with a strong diminution of high frequency noise  
244 suggesting a drift of the temperature sensor. Consequently these temperature data were

245 rejected from the time-series analysis. The potential temperature/salinity diagram is compared  
246 to KEOPS1 and KEOPS2 CTD downcast at station A3 (Fig. 4). The CTD sensor recorded the  
247 signature of the UCDW and no intrusion of overlying WW could be detected.

248 The power spectrum of vertical sediment trap displacements identified six significant  
249 peaks corresponding to frequencies of 6.2 h, 8.2 h, 23.9 h, 25.7 h and 14 days (Fig 5a).  
250 Concomitant peaks of depth, angle and current speed were also observed with a period of 14  
251 days. However, spectral analysis of the potential density anomaly  $\sigma_\theta$  revealed only one  
252 significant major power peak corresponding to a frequency of 12.4 h (Fig. 5b). Isopycnal  
253 displacements were driven by the unique tidal component (M2, 12.4h period) and trap  
254 displacements resulted from a complex combination of multiple tidal components. The power  
255 spectrum analysis suggested that a 40 hour window was relevant to filter out most of the short  
256 term variability (black line in Fig 3a – 3e).

257 A pseudo-lagrangian trajectory was calculated by cumulating the instantaneous current  
258 vectors (Fig 6). Over short time-scales (hours to day) the trajectory displays numerous tidal  
259 ellipses. The flow direction is mainly to the South-East in October 2011 to December 2012  
260 and North-East from December 2011 to April 2012. For the entire current meter record (6  
261 months) the overall displacement followed a 120 km northeasterly, anticlockwise trajectory  
262 with an integrated current speed of approximately  $1 \text{ cm s}^{-1}$ .

### 263 **3.2 Seasonality of surface chlorophyll *a* concentration above trap location**

264 The seasonal variations of surface chlorophyll *a* concentration for the sediment trap  
265 deployment period differed significantly from the long-term climatology (Fig 7a). The bloom  
266 started at the beginning of November 2011, ten days after the start of the sediment trap  
267 deployment. Maximum surface chlorophyll *a* values of  $2.5 \mu\text{g L}^{-1}$  occurred on the first week  
268 of November and subsequently declined rapidly to  $0.2 \mu\text{g L}^{-1}$  in late December 2011. A

269 second increase in surface chlorophyll *a* up to 1  $\mu\text{g L}^{-1}$  occurred in January 2012 and values  
270 decreased to winter levels of 0.2  $\mu\text{g L}^{-1}$  in February 2012. A short-term increase of 0.8  $\mu\text{g L}^{-1}$   
271 occurred in mid-April 2012.

### 272 **3.3 Swimmer abundances**

273 No swimmers were found in cups #3 and #5 (Table 2). Total swimmer numbers were highest  
274 in winter (1544 individuals in cup #12). When normalized to cup opening time, swimmer  
275 intrusion rates were highest between mid-December 2011 and mid-February 2012 (from 26 to  
276 55 individuals  $\text{d}^{-1}$ ) and lower than 20 individuals  $\text{d}^{-1}$  for the remainder of the year. Swimmers  
277 were numerically dominated by copepods throughout the year, but elevated amphipod and  
278 pteropod abundances were observed at the end of January and February 2012 (Table 2). There  
279 was no significant correlation between mass flux, POC and PON fluxes and total swimmer  
280 number or intrusion rate (Spearman's correlation test,  $p > 0,01$ ). Copepods were essentially  
281 small cyclopid species. Amphipods were predominantly represented by the hyperidean  
282 *Cylopus magellanicus* and *Themisto gaudichaudii*. Pteropods were represented by *Clio*  
283 *pyramidata*, *Limacina helicina* forma *antarctica* and *Limacina retroversa* subsp. *australis*.  
284 Euphausiids were only represented by the genus *Thysanoessa*. One *Slapa thompsoni* salp  
285 (aggregate form) was found in the last winter cup #12.

### 286 **3.4 Seasonal particulate organic carbon and nitrogen fluxes**

287 Particulate organic carbon flux ranged from 0.15 to 0.55  $\text{mmol m}^{-2} \text{d}^{-1}$  during the productive  
288 period except during two short export events of  $1.6 \pm 0.04$  and  $1.5 \pm 0.04$   $\text{mmol m}^{-2} \text{d}^{-1}$   
289 sampled in cups #4 (2 to 12 December 2011) and #9 (25 January to 8 February 2012),  
290 respectively (Fig. 7b). The two flux events occurred with an approximate time lag of one  
291 month compared to peaks in surface chlorophyll *a* values. A modest value of  $0.27 \pm 0.01$   $\text{mmol}$   
292  $\text{m}^{-2} \text{d}^{-1}$  was observed in autumn (cup #11, 22 February to 30 May 2012). The lowest POC flux

293 was measured during winter ( $0.04 \text{ mmol m}^{-2} \text{ d}^{-1}$ , cup #12, 31 May to 7 October). Assuming  
294 that POC export was negligible from mid September to mid October, the annually integrated  
295 POC flux was  $98.2 \pm 4.4 \text{ mmol m}^{-2} \text{ y}^{-1}$  (Table 1). The two short (<14 days) export events  
296 accounted for  $16.2 \pm 0.5 \%$  (cup #4) and  $21.0 \pm 0.6 \%$  (cup #9) of the annual carbon export out  
297 of the mixed layer (Table 1). Mass percentage of organic carbon ranged from 3.3 % to 17.4 %  
298 (Fig. 7b). Values were slightly higher in autumn and winter (respectively  $13.1 \pm 0.2 \%$  and  
299  $11 \pm 2.1 \%$  in cups #11 and #12) than in the summer, with the exception of cup #5 where the  
300 highest value of 17.4 % was observed. PON fluxes followed the same seasonal patterns as  
301 POC. This resulted in a relatively stable POC:PON ratio that varied between 6.1 to 7.4, except  
302 in the autumn cup #11 where it exceeded 8.1 (Table 1).

## 303 **4 Discussion**

### 304 **4.1 Physical conditions of trap deployment**

305 Moored sediment traps can be subject to hydrodynamic biases that affect the accuracy of  
306 particle collection (Buesseler et al., 2007a). The aspect ratio, tilt and horizontal flow regimes  
307 are important considerations when assessing sediment trap performance. Specifically, the line  
308 angle and aspect ratio of cylindrical traps can result in oversampling (Hawley, 1988).  
309 Horizontal current velocities of  $12 \text{ cm s}^{-1}$  are often invoked as a critical threshold over which  
310 particles are no longer quantitatively sampled (Baker et al., 1988). During the sediment trap  
311 deployment period we observed generally low current speeds (mean  $< 10 \text{ cm s}^{-1}$ ) with 75% of  
312 the recorded data lower than  $12 \text{ cm s}^{-1}$ . Despite the high aspect ratio of the PPS3 trap (4.75),  
313 and the small mooring line angle deviations, it is likely that episodic increases in current  
314 velocities ( $>12 \text{ cm s}^{-1}$ ) impacted collection efficiency. When integrated over the entire current  
315 meter record (October 2011 to April 2012), the resulting flow is consistent with the annual

316 northeastward, low velocity ( $\sim 1 \text{ cm s}^{-1}$ ) geostrophic flow previously reported over the  
317 central part of the Kerguelen plateau (Park et al., 2008b).

318         The depth of the winter mixed layer (WML) on the Kerguelen Plateau is usually  
319 shallower than 250 m (Park et al., 1998; Metzl et al., 2006). The sediment trap deployment  
320 depth of  $\sim 300$  m was selected to sample particle flux exiting the WML. The moored CTD  
321 sensor did not record any evidence of a winter water incursion during the deployment period,  
322 confirming the WML did not reach the trap depth. The small depth variations observed during  
323 the deployment period resulted from vertical displacement of the trap. Variations of  $\sigma_\theta$  may  
324 have resulted from both vertical displacement of the CTD sensor and possible isopycnal  
325 displacements due to strong internal waves that can occur with an amplitude of  $> 50$  m at this  
326 depth (Park et al., 2008a). Our measurements demonstrate that isopycnal displacements are  
327 consistent with the M2 (moon 2, 12.4 h period) tidal forcing described in physical modeling  
328 studies (Maraldi et al., 2009, 2011). Spectral analysis indicates that high frequency tidal  
329 currents are the major circulation components. Time-integrated currents suggest that  
330 advection is weak and occurs over longer timescale (months). Assuming the current flow  
331 measured at the sediment trap deployment depth is representative of the prevailing current  
332 under the WML, more than three months are required for particles to leave the plateau from  
333 the A3 station, a timescale larger than the bloom duration itself. Therefore we consider that  
334 the particles collected in the sediment trap at station A3 were produced in the surface waters  
335 located above the plateau during bloom conditions.

#### 336         **4.2 Swimmers and particle solubilization**

337         Aside from the hydrodynamic effects discussed above, other potential biases characterizing  
338 sediment trap deployments, particularly those in shallow waters, is the presence of swimmers  
339 and particle solubilization. Swimmers can artificially increase POC fluxes by entering the

340 cups and releasing particulate organic matter or decrease the flux by feeding in the trap funnel  
341 (Buesseler et al., 2007a). Some studies have focused specifically on swimmer communities  
342 collected in shallow sediment traps (Matsuno et al., 2014 and references therein) although trap  
343 collection of swimmers is probably selective and therefore not quantitative. Total swimmer  
344 intrusion rate was highest in cups #6 to #9 (December 2011 to February 2012) generally  
345 through the representation of copepods and amphipods (Table 2). The maximum swimmer  
346 intrusion rate in mid-summer as well as the copepod dominance is consistent with the fourfold  
347 increase in mesozooplankton abundance observed from winter to summer (Carlotti et al.,  
348 2014). Swimmer abundance was not correlated with mass flux, POC or PON fluxes,  
349 suggesting that their presence did not systematically affect particulate fluxes inside the cups.  
350 Nevertheless such correlations cannot rule out the possibility of swimmers feeding in the trap  
351 funnel modifying particle flux collection.

352         Particle solubilization in preservative solutions may also lead to an underestimation of  
353 total flux measured in sediment traps. Previous analyses from traps poisoned with mercuric  
354 chloride suggest that ~30 % of total organic carbon flux can be found in the dissolved phase  
355 and much higher values of 50 % and 90 % may be observed for nitrogen and phosphorous,  
356 respectively (Antia, 2005; O'Neill et al., 2005). Unfortunately the use of a formaldehyde-  
357 based preservative in our trap samples precludes any direct estimate of excess of dissolved  
358 organic carbon in the sample cup supernatant. Furthermore, corrections for particle leaching  
359 have been considered problematic in the presence of swimmers since a fraction of the  
360 leaching may originate from the swimmers themselves (Antia, 2005), potentially leading to  
361 over-correction. Particles solubilization may have occurred in our samples as evidenced by  
362 excess  $\text{PO}_4^{3-}$  in the supernatant. However the largest values were measured in sample cups  
363 where total swimmers were abundant (cups #8 to #12, data not shown). Consequently, it was  
364 not possible to discriminate solubilisation of P from swimmers and passively settling particles



365 and it therefore remains difficult to quantify the effect of particle leaching. However, leaching  
366 of POC should be less problematic in formalin-preserved samples because aldehydes fix  
367 organic matter, in addition to poisoning microbial activity.

### 368 **4.3 Seasonal dynamics of POC export**

369 The sediment trap record obtained from station A3 provides the first direct estimate of POC  
370 export covering an entire season over the naturally fertilized Kerguelen Plateau. We observed  
371 a temporal lag of one month between the two surface chlorophyll *a* peaks and the two export  
372 events. Based on a compilation of annual sediment trap deployments, Lutz et al. (2007)  
373 reported that export quickly follows primary production at low latitudes whereas a time lag up  
374 to two months could occur at higher latitudes. A 1-2 month lag was observed between  
375 production and export in the Pacific sector of the Southern Ocean (Buesseler et al., 2001), as  
376 well as along 170°W (Honjo et al., 2000) and in the Australian sector of the Subantarctic  
377 Zone (Rigual-Hernández et al., 2015). The temporal lag between surface production and  
378 measured export in deep traps can originate from ecological processes in the upper ocean (e.g.  
379 carbon retention in the mixed layer) as well as slow sinking velocities (Armstrong et al.,  
380 2009) and one cannot differentiate the two processes from a single deep trap signal. A global-  
381 scale modeling study suggests that the strongest temporal decoupling between production and  
382 export (more than one month) occurs in areas characterized by a strong seasonal variability in  
383 primary production (Henson et al., 2014). The study attributes this decoupling to differences  
384 in phenology of phytoplankton and zooplankton and evokes zooplankton ejection products as  
385 major contributors to fast sinking particles sedimenting post bloom.

386 On the Kerguelen Plateau there is evidence that a significant fraction of  
387 phytoplankton biomass comprising the two chlorophyll peaks is remineralized by a highly  
388 active heterotrophic microbial community (Obernosterer et al., 2008; Christaki et al., 2014).  
389 Another fraction is likely channeled toward higher trophic levels through the intense grazing

390 pressure that support the observed increase in zooplankton biomass (Carlotti et al., 2008,  
391 2014). Therefore an important fraction of phytoplankton biomass increases observed by  
392 satellite may not contribute to export fluxes. Notably, the POC:PON ratio measured in our  
393 trap material is close to values reported for marine diatoms ( $7.3 \pm 1.2$ , Sarthou et al., 2005),  
394 compared to the C:N ratio of zooplankton faecal pellets which is typically higher (7.3 to >15,  
395 Gerber and Gerber, 1979; Checkley and Entzeroth, 1985; Morales, 1987). Simple mass  
396 balance would therefore suggest a significant contribution of phytoplanktonic cells to the  
397 POC export, which is indeed corroborated by detailed microscopic analysis (Rembauville et  
398 al., 2014).

399         Although we observed increasing contribution of faecal pellet carbon post-bloom  
400 (Rembauville et al., 2014), in line with the model output of Henson et al. (2014), differences  
401 in phytoplankton and zooplankton phenology do not fully explain the seasonality of export on  
402 the Kerguelen Plateau. Considering the shallow trap depth (289 m) and typical sinking speed  
403 of  $100 \text{ m d}^{-1}$  for phyto-aggregates (Allredge and Gotschalk, 1988; Peterson et al., 2005; Trull  
404 et al., 2008a), aggregate-driven export following bloom demise would suggest a short lag of a  
405 few days between production and export peaks. The temporal lag of one month measured in  
406 the present study suggest either slow sinking rates ( $<5 \text{ m d}^{-1}$ ) characteristic of single  
407 phytoplanktonic cells or faster sinking particles that originate from sub-surface production  
408 peaks undetected by satellite. It is generally accepted that satellite detection depth is 20-50 m  
409 (Gordon and McCluney, 1975), and can be less than 20 m when surface chlorophyll *a* exceed  
410  $0.2 \mu\text{g L}^{-1}$  (Smith, 1981), which prevents the detection of deep phytoplanktonic biomass  
411 structures (Villareal et al., 2011). Although subsurface chlorophyll maximum located around  
412 100 m have been observed over the Kerguelen Plateau at the end of the productive period,  
413 they have been interpreted to result from the accumulation of surface production at the base of  
414 the mixed layer rather than a subsurface productivity feature (Uitz et al., 2009). In support of

415 this detailed taxonomic analysis of the exported material highlight diatom resting spores as  
416 major contributors to the two export fluxes rather than a composite surface community  
417 accumulated at the base of the mixed layer. The hypothesis of a mass production of nutrient-  
418 limited resting spores post-bloom with high settling rates explains the temporal patterns of  
419 export we observed (Rembauville et al., 2014). However a better knowledge of the dynamics  
420 of factors responsible for resting spore formation by diatoms remains necessary to fully  
421 validate this hypothesis.

#### 422 **4.4 Evidence for significant flux attenuation over the Kerguelen Plateau**

423 The Kerguelen Plateau annual POC export ( $98.2 \pm 4.4 \text{ mmol m}^{-2} \text{ y}^{-1}$ ) approaches the median  
424 global ocean POC export value comprising shallow and deep sediment traps ( $83 \text{ mmol m}^{-2} \text{ y}^{-1}$ ,  
425 Lampitt and Antia, 1997), but is also close to values observed in HNLC areas of the POOZ  
426 ( $11\text{-}43 \text{ mmol m}^{-2} \text{ y}^{-1}$  at 500 m, Fischer et al., 2000). Moreover, the magnitude of annual POC  
427 export measured at  $\sim 300\text{m}$  on the Kerguelen Plateau is comparable to deep-ocean ( $>2 \text{ km}$ )  
428 POC fluxes measured from the iron-fertilized Crozet ( $60 \text{ mmol m}^{-2} \text{ y}^{-1}$ , Salter et al., 2012) and  
429 South Georgia blooms ( $180 \text{ mmol m}^{-2} \text{ y}^{-1}$ , Manno et al., 2014).

430 We first compared the sediment trap export fluxes with short-term estimates at 200 m  
431 in spring (KEOPS2) and summer (KEOPS1). The POC flux recorded in the moored sediment  
432 trap represents only a small fraction (3-8%) of the POC flux measured at the base of the  
433 winter mixed layer (200 m) by different approaches during the spring KEOPS2 cruise (Table  
434 3). The same conclusion can be drawn when considering the comparison with different  
435 estimates made at the end of summer during KEOPS1. Moreover, the annual POC export of  
436  $\sim 0.1 \text{ mol m}^{-2} \text{ y}^{-1}$  at 289 m (Table 1) represents only 2% of the indirect estimate of POC export  
437 ( $5.1 \text{ mol m}^{-2} \text{ y}^{-1}$ ) at the base of the WML (200 m) on the Kerguelen Plateau based on a  
438 seasonal DIC budget (Blain et al., 2007). The short term estimates are derived from a diverse  
439 range of methods. The  $^{234}\text{Th}$  proxy is based on the  $^{234}\text{Th}$  deficit relative to the  $^{238}\text{U}$  due to its

440 adsorption on particles, and its subsequent conversion to carbon fluxes using measured  
441 POC:<sup>234</sup>Th ratios. (Coale and Bruland, 1985; Buesseler et al., 2006; Savoye et al., 2006). The  
442 UVP provides high resolution images of particles (>52 µm) and the particle size distribution  
443 is then converted to carbon fluxes using an empirical relationship (Guidi et al., 2008; Picheral  
444 et al., 2010). Drifting gel traps allow the collection, preservation and imaging of sinking  
445 particles (>71 µm) that are converted to carbon fluxes using empirical volume:carbon  
446 relationship (Ebersbach and Trull, 2008; Ebersbach et al., 2011; Laurenceau-Cornec et al.,  
447 2015). Finally, drifting sediment traps are conceptually similar to moored sediment traps but  
448 avoid most of the hydrodynamic biases associated with this technique (Buesseler et al.,  
449 2007a). The diversity of the methods and differences in depth where the POC flux was  
450 estimated render quantitative comparisons challenging. Nevertheless, POC fluxes measured at  
451 289 m with the moored sediment trap are considerably lower than other estimates made at 200  
452 m. This result indicates either extremely rapid attenuation of flux between 200 m and 300 m  
453 or significant sampling bias by the sediment trap.

454 We note that low carbon export fluxes around 300 m have been previously reported on  
455 the Kerguelen Plateau. In spring 2011, UVP derived estimates of POC export at 350 m are 0.1  
456 to 0.3 mmol m<sup>-2</sup> d<sup>-1</sup> (Table 3), a value close to our reported value of 0.15 mmol m<sup>-2</sup> d<sup>-1</sup>. In  
457 summer 2005, POC export at 330 m from gel trap is 0.7 mmol m<sup>-2</sup> d<sup>-1</sup> (Ebersbach and Trull  
458 2008), which is also close to our value of 1.5 mmol m<sup>-2</sup> d<sup>-1</sup>. Using the Jouandet et al. (2014)  
459 data at 200 m (1.9 mmol m<sup>-2</sup> d<sup>-1</sup>) and 350 m (0.3 mmol m<sup>-2</sup> d<sup>-1</sup>) and the Ebersbach and Trull  
460 (2008) data at 200 m (5.2 mmol m<sup>-2</sup> d<sup>-1</sup>) and 330 m (0.7 mmol m<sup>-2</sup> d<sup>-1</sup>) leads to Martin power  
461 law exponents values of 3.3 and 4, respectively. These values are high when compared to the  
462 range of 0.4–1.7 that was initially compiled for the global ocean (Buesseler et al., 2007b).  
463 However, there is increasing evidence in support of much higher b-values in the Southern  
464 Ocean that fall in the range 0.9-3.9 (Lam and Bishop, 2007; Henson et al., 2012; Cavan et al.,

465 2015). Our calculations are thus consistent with emerging observations of significant POC  
466 flux attenuation in the Southern Ocean.

467 Using the aforementioned  $b$  values (3.3 and 4) and the POC flux derived from  $^{234}\text{Th}$   
468 deficit at 200 m in spring (Planchon et al., 2014), we estimate POC fluxes at 289 m of 0.7 to  
469  $1.1 \text{ mmol m}^{-2} \text{ d}^{-1}$ . The flux measured in our sediment trap ( $0.15 \text{ mmol m}^{-2} \text{ d}^{-1}$ ) data represents  
470 14 % to 21 % of this calculated flux. Very similar percentages (21 % to 27 %) are found using  
471 the POC fluxes derived from the  $^{234}\text{Th}$  deficit in summer (Savoie et al., 2008). Therefore we  
472 consider that the moored sediment trap collected ~15-30 % of the  $^{234}\text{Th}$  – derived particle flux  
473 equivalent throughout the year. Trap-derived particle fluxes can represent 0.1 to >3 times the  
474  $^{234}\text{Th}$ -derived particles in shallow sediment traps (Buesseler, 1991; Buesseler et al., 1994;  
475 Coppola et al., 2002; Gustafsson et al., 2004) and this difference is largely attributed to the  
476 sum of hydrodynamic biases and swimmer activities (Buesseler, 1991), although it probably  
477 also includes the effect of post-collection particle solubilisation. In the Antarctic Peninsula,  
478  $^{234}\text{Th}$  derived POC export was 20 times higher than the fluxes collected by a shallow,  
479 cylindrical, moored sediment trap at 170 m (Buesseler et al., 2010). The present deployment  
480 context is less extreme (depth of 289 m, mean current speed  $<10 \text{ cm s}^{-1}$ , low tilt angle, high  
481 aspect ratio of the cylindrical PPS3 trap) but we consider that hydrodynamics (current speed  
482 higher than  $12 \text{ cm s}^{-1}$  during short tidal-driven events) and possible zooplankton feeding on  
483 the trap funnel are potential biases that may explain in part the low fluxes recorded by the  
484 moored sediment trap. Therefore the low fluxes observed likely result from a combined effect  
485 of collection bias (hydrodynamics and swimmers) and attenuation of the POC flux between  
486 the base of the WML and 300 m. However, it is not possible with the current dataset to isolate  
487 a specific explanation for low flux values.

488 Strong POC flux attenuation over the Kerguelen Plateau compared to the open ocean  
489 is also reported by Laurenceau-Cornec et al. (2015) who associate this characteristic to a

490 HBLE scenario and invoke the role of mesozooplankton in the carbon flux attenuation.  
491 Between October and November 2011, mesozooplankton biomass in the mixed layer doubled  
492 (Carlotti et al., 2014) and summer biomass was twofold higher still (Carlotti et al., 2008).  
493 These seasonal patterns are consistent with the maximum swimmer intrusion rate and  
494 swimmer diversity observed in summer (Table 2). It has previously been concluded that  
495 zooplankton biomass is more tightly coupled to phytoplankton biomass on the plateau  
496 compared to oceanic waters, leading to higher secondary production on the plateau (Carlotti et  
497 al., 2008, 2014). Further support linking zooplankton dynamics to HBLE environments of  
498 iron-fertilized blooms are the findings of Cavan et al. (2015) that documents the lowest export  
499 ratio (exported production/primary production) in the most productive, naturally fertilized  
500 area downstream of South Georgia. Another important ecosystem feature associated to the  
501 HBLE environment of the Kerguelen Plateau, and likely shared by other island-fertilized  
502 blooms in the Southern Ocean, is the presence of mesopelagic fish (myctophid spawning and  
503 larvae foraging site, Koubbi et al., 1991, 2001). Mesopelagic fish can be tightly coupled to  
504 lower trophic levels (Saba and Steinberg, 2012) and can play a significant role in carbon flux  
505 attenuation (Davison et al., 2013). Although important for carbon budgets it is a compartment  
506 often neglected due to the challenge of quantitative sampling approaches. We suggest that the  
507 HBLE scenario and large attenuation of carbon flux beneath the WML at Kerguelen may  
508 represents the transfer of carbon biomass to higher and mobile trophic groups that fuel large  
509 mammal and bird populations rather than the classical remineralization-controlled vertical  
510 attenuation characterizing open ocean environments. Although technically challenging,  
511 testing this hypothesis should be a focus for future studies in this and similar regions.

## 512 **5. Conclusion**

513 We report the seasonal dynamics of particulate organic carbon (POC) export under the winter  
514 mixed layer (289 m) of the naturally iron fertilized and productive central Kerguelen Plateau.

515 Annual POC flux was remarkably low ( $98 \text{ mmol m}^{-2}$ ) and occurred primarily during two  
516 episodic (<14 days) flux events exported with a 1 month lag following two surface  
517 chlorophyll *a* peaks. Analysis of the hydrological conditions and a comparison with different  
518 estimates of POC fluxes in spring and summer at the same station suggests that the sediment  
519 trap was subject to possible hydrodynamic and biological biases leading to under collection of  
520 particle flux. Nevertheless the low POC export was close to other estimates of deep (>300 m)  
521 POC export at the same station and is consistent with high attenuation coefficients reported  
522 from other methods. We invoke heterotrophic microbial activity and mesozooplankton and  
523 mesopelagic fish activity as possible explanations for efficient carbon flux attenuation and/or  
524 transfer to higher trophic levels which results in a High Biomass, Low Export environment.

525 The biogenic silicon, diatoms assemblages and faecal pellet fluxes are reported in a  
526 companion paper that identifies the primary ecological vectors regulating the magnitude of  
527 POC export and seasonal patterns in BSi:POC export (Rembauville et al., 2014).

## 528 **Acknowledgements**

529 We thank the Chief Scientist Prof. Bernard Quéguiner, the Captain Bernard Lassiette and his  
530 crew during the KEOPS2 mission on the R/V Marion Dufresne II. We thank Leanne Armand  
531 and Tom Trull for their constructive comments, as well as three anonymous reviewers which  
532 helped us to improve the manuscript. This work was supported by the French Research  
533 program of INSU-CNRS LEFE-CYBER (Les enveloppes fluides et l'environnement – Cycles  
534 biogéochimiques, environnement et ressources), the French ANR (Agence Nationale de la  
535 Recherche, SIMI-6 program, ANR-10-BLAN-0614), the French CNES (Centre National  
536 d'Etudes Spatiales) and the French Polar Institute IPEV (Institut Polaire Paul-Emile Victor).

- 538 Allredge, A.L., Gotschalk, C., 1988. In situ settling behavior of marine snow. *Limnol. Oceanogr.* 33, 339–351.
- 539 Aminot, A., Kerouel, R., 2007. Dosage automatique des nutriments dans les eaux marines: méthodes en flux  
540 continu. Ifremer, Plouzané, France.
- 541 Antia, A.N., 2005. Solubilization of particles in sediment traps: revising the stoichiometry of mixed layer export.  
542 *Biogeosciences* 2, 189–204. doi:10.5194/bg-2-189-2005
- 543 Armstrong, R.A., Peterson, M.L., Lee, C., Wakeham, S.G., 2009. Settling velocity spectra and the ballast ratio  
544 hypothesis. *Deep Sea Res. Part II Top. Stud. Oceanogr.* 56, 1470–1478. doi:10.1016/j.dsr2.2008.11.032
- 545 Arrigo, K.R., Worthen, D., Schnell, A., Lizotte, M.P., 1998. Primary production in Southern Ocean waters. *J.*  
546 *Geophys. Res. Oceans* 103, 15587–15600. doi:10.1029/98JC00930
- 547 Baker, E.T., Milburn, H.B., Tennant, D.A., 1988. Field assessment of sediment trap efficiency under varying  
548 flow conditions. *J. Mar. Res.* 46, 573–592. doi:10.1357/002224088785113522
- 549 Barbeau, K., Moffett, J.W., Caron, D.A., Croot, P.L., Erdner, D.L., 1996. Role of protozoan grazing in relieving  
550 iron limitation of phytoplankton. *Nature* 380, 61–64. doi:10.1038/380061a0
- 551 Batten, S.D., Gower, J.F.R., 2014. Did the iron fertilization near Haida Gwaii in 2012 affect the pelagic lower  
552 trophic level ecosystem? *J. Plankton Res.* 36, 925–932. doi:10.1093/plankt/fbu049
- 553 Blain, S., Quéguiner, B., Armand, L., Belviso, S., Bombled, B., Bopp, L., Bowie, A., Brunet, C., Brussaard, C.,  
554 Carloti, F., Christaki, U., Corbière, A., Durand, I., Ebersbach, F., Fuda, J.-L., Garcia, N., Gerringa, L.,  
555 Griffiths, B., Guigue, C., Guillermin, C., Jaquet, S., Jeandel, C., Laan, P., Lefèvre, D., Lo Monaco, C.,  
556 Malits, A., Mosseri, J., Obernosterer, I., Park, Y.-H., Picheral, M., Pondaven, P., Remenyi, T.,  
557 Sandroni, V., Sarthou, G., Savoye, N., Scouarnec, L., Souhaut, M., Thuiller, D., Timmermans, K.,  
558 Trull, T., Uitz, J., van Beek, P., Veldhuis, M., Vincent, D., Viollier, E., Vong, L., Wagener, T., 2007.  
559 Effect of natural iron fertilization on carbon sequestration in the Southern Ocean. *Nature* 446, 1070–  
560 1074. doi:10.1038/nature05700
- 561 Blain, S., Tréguer, P., Belviso, S., Bucciarelli, E., Denis, M., Desabre, S., Fiala, M., Martin Jézéquel, V., Le  
562 Fèvre, J., Mayzaud, P., Marty, J.-C., Razouls, S., 2001. A biogeochemical study of the island mass  
563 effect in the context of the iron hypothesis: Kerguelen Islands, Southern Ocean. *Deep Sea Res. Part*  
564 *Oceanogr. Res. Pap.* 48, 163–187. doi:10.1016/S0967-0637(00)00047-9
- 565 Boltovskoy, D., 1999. South Atlantic zooplankton. *Backhuys*.
- 566 Bopp, L., Kohfeld, K.E., Le Quééré, C., Aumont, O., 2003. Dust impact on marine biota and atmospheric CO<sub>2</sub>  
567 during glacial periods. *Paleoceanography* 18, 1046. doi:10.1029/2002PA000810
- 568 Boyd, P.W., Jickells, T., Law, C.S., Blain, S., Boyle, E.A., Buesseler, K.O., Coale, K.H., Cullen, J.J., Baar,  
569 H.J.W. de, Follows, M., Harvey, M., Lancelot, C., Levasseur, M., Owens, N.P.J., Pollard, R., Rivkin,  
570 R.B., Sarmiento, J., Schoemann, V., Smetacek, V., Takeda, S., Tsuda, A., Turner, S., Watson, A.J.,  
571 2007. Mesoscale Iron Enrichment Experiments 1993–2005: Synthesis and Future Directions. *Science*  
572 315, 612–617. doi:10.1126/science.1131669
- 573 Boyd, P.W., Law, C.S., Hutchins, D.A., Abraham, E.R., Croot, P.L., Ellwood, M., Frew, R.D., Hadfield, M.,  
574 Hall, J., Handy, S., Hare, C., Higgins, J., Hill, P., Hunter, K.A., LeBlanc, K., Maldonado, M.T., McKay,  
575 R.M., Mioni, C., Oliver, M., Pickmere, S., Pinkerton, M., Safi, K., Sander, S., Sanudo-Wilhelmy, S.A.,  
576 Smith, M., Strzepek, R., Tovar-Sanchez, A., Wilhelm, S.W., 2005. FeCycle: Attempting an iron  
577 biogeochemical budget from a mesoscale SF<sub>6</sub> tracer experiment in unperturbed low iron waters. *Glob.*  
578 *Biogeochem. Cycles* 19, GB4S20. doi:10.1029/2005GB002494
- 579 Boyd, P.W., Trull, T.W., 2007. Understanding the export of biogenic particles in oceanic waters: Is there  
580 consensus? *Prog. Oceanogr.* 72, 276–312. doi:10.1016/j.pocean.2006.10.007
- 581 Buesseler, K.O., 1991. Do upper-ocean sediment traps provide an accurate record of particle flux? *Nature* 353,  
582 420–423. doi:10.1038/353420a0
- 583 Buesseler, K.O., Antia, A.N., Chen, M., Fowler, S.W., Gardner, W.D., Gustafsson, Ö., Harada, K., Michaels,  
584 A.F., Rutgers v. d. Loeff, M., Sarin, M., Steinberg, D.K., Trull, T., 2007a. An assessment of the use of  
585 sediment traps for estimating upper ocean particle fluxes. *J. Mar. Res.* 65, 345–416.
- 586 Buesseler, K.O., Ball, L., Andrews, J., Cochran, J.K., Hirschberg, D.J., Bacon, M.P., Flear, A., Brzezinski, M.,  
587 2001. Upper ocean export of particulate organic carbon and biogenic silica in the Southern Ocean along  
588 170°W. *Deep Sea Res. Part II Top. Stud. Oceanogr.* 48, 4275–4297. doi:10.1016/S0967-  
589 0645(01)00089-3
- 590 Buesseler, K.O., Benitez-Nelson, C.R., Moran, S.B., Burd, A., Charette, M., Cochran, J.K., Coppola, L., Fisher,  
591 N.S., Fowler, S.W., Gardner, W.D., Guo, L.D., Gustafsson, Ö., Lamborg, C., Masque, P., Miquel, J.C.,  
592 Passow, U., Santschi, P.H., Savoye, N., Stewart, G., Trull, T., 2006. An assessment of particulate  
593 organic carbon to thorium-234 ratios in the ocean and their impact on the application of <sup>234</sup>Th as a  
594 POC flux proxy. *Mar. Chem., Future Applications of <sup>234</sup>Th in Aquatic Ecosystems (FATE)* 100, 213–  
595 233. doi:10.1016/j.marchem.2005.10.013



596 Buesseler, K.O., Boyd, P.W., 2009. Shedding light on processes that control particle export and flux attenuation  
597 in the twilight zone of the open ocean. *Limnol. Oceanogr.* 54, 1210–1232.  
598 doi:10.4319/lo.2009.54.4.1210

599 Buesseler, K.O., Lamborg, C.H., Boyd, P.W., Lam, P.J., Trull, T.W., Bidigare, R.R., Bishop, J.K.B., Casciotti,  
600 K.L., Dehairs, F., Elskens, M., Honda, M., Karl, D.M., Siegel, D.A., Silver, M.W., Steinberg, D.K.,  
601 Valdes, J., Mooy, B.V., Wilson, S., 2007b. Revisiting Carbon Flux Through the Ocean's Twilight Zone.  
602 *Science* 316, 567–570. doi:10.1126/science.1137959

603 Buesseler, K.O., McDonnell, A.M.P., Schofield, O.M.E., Steinberg, D.K., Ducklow, H.W., 2010. High particle  
604 export over the continental shelf of the west Antarctic Peninsula. *Geophys. Res. Lett.* 37, L22606.  
605 doi:10.1029/2010GL045448

606 Buesseler, K.O., Michaels, A.F., Siegel, D.A., Knap, A.H., 1994. A three dimensional time-dependent approach  
607 to calibrating sediment trap fluxes. *Glob. Biogeochem. Cycles* 8, 179–193. doi:10.1029/94GB00207

608 Carlotti, F., Thibault-Botha, D., Nowaczyk, A., Lefèvre, D., 2008. Zooplankton community structure, biomass  
609 and role in carbon fluxes during the second half of a phytoplankton bloom in the eastern sector of the  
610 Kerguelen Shelf (January–February 2005). *Deep Sea Res. Part II Top. Stud. Oceanogr.* 55, 720–733.  
611 doi:10.1016/j.dsr2.2007.12.010

612 Cavan, E.L., Le Moigne, F. a. c., Poulton, A.J., Tarling, G.A., Ward, P., Daniels, C.J., Fragoso, G., Sanders, R.J.,  
613 2015. Zooplankton fecal pellets control the attenuation of particulate organic carbon flux in the Scotia  
614 Sea, Southern Ocean. *Geophys. Res. Lett.* 2014GL062744. doi:10.1002/2014GL062744

615 Checkley, D.M., Entzeroth, L.C., 1985. Elemental and isotopic fractionation of carbon and nitrogen by marine,  
616 planktonic copepods and implications to the marine nitrogen cycle. *J. Plankton Res.* 7, 553–568.  
617 doi:10.1093/plankt/7.4.553

618 Christaki, U., Lefèvre, D., Georges, C., Colombet, J., Catala, P., Courties, C., Sime-Ngando, T., Blain, S.,  
619 Obernosterer, I., 2014. Microbial food web dynamics during spring phytoplankton blooms in the  
620 naturally iron-fertilized Kerguelen area (Southern Ocean). *Biogeosciences* 11, 6739–6753.  
621 doi:10.5194/bg-11-6739-2014

622 Coale, K.H., Bruland, K.W., 1985.  $^{234}\text{Th}$  Disequilibria Within the California Current. *Limnol.*  
623 *Oceanogr.* 30, 22–33.

624 Coale, K.H., Johnson, K.S., Chavez, F.P., Buesseler, K.O., Barber, R.T., Brzezinski, M.A., Cochlan, W.P.,  
625 Millero, F.J., Falkowski, P.G., Bauer, J.E., Wanninkhof, R.H., Kudela, R.M., Altabet, M.A., Hales,  
626 B.E., Takahashi, T., Landry, M.R., Bidigare, R.R., Wang, X., Chase, Z., Strutton, P.G., Friederich,  
627 G.E., Gorbunov, M.Y., Lance, V.P., Hiltling, A.K., Hiscock, M.R., Demarest, M., Hiscock, W.T.,  
628 Sullivan, K.F., Tanner, S.J., Gordon, R.M., Hunter, C.N., Elrod, V.A., Fitzwater, S.E., Jones, J.L.,  
629 Tozzi, S., Koblizek, M., Roberts, A.E., Herndon, J., Brewster, J., Ladizinsky, N., Smith, G., Cooper, D.,  
630 Timothy, D., Brown, S.L., Selph, K.E., Sheridan, C.C., Twining, B.S., Johnson, Z.I., 2004. Southern  
631 Ocean Iron Enrichment Experiment: Carbon Cycling in High- and Low-Si Waters. *Science* 304, 408–  
632 414. doi:10.1126/science.1089778

633 Coppola, L., Roy-Barman, M., Wassmann, P., Mulrow, S., Jeandel, C., 2002. Calibration of sediment traps and  
634 particulate organic carbon export using  $^{234}\text{Th}$  in the Barents Sea. *Mar. Chem.* 80, 11–26.  
635 doi:10.1016/S0304-4203(02)00071-3

636 Davison, P.C., Checkley Jr., D.M., Koslow, J.A., Barlow, J., 2013. Carbon export mediated by mesopelagic  
637 fishes in the northeast Pacific Ocean. *Prog. Oceanogr.* 116, 14–30. doi:10.1016/j.pocean.2013.05.013

638 De Baar, H.J.W., Boyd, P.W., Coale, K.H., Landry, M.R., Tsuda, A., Assmy, P., Bakker, D.C.E., Bozec, Y.,  
639 Barber, R.T., Brzezinski, M.A., Buesseler, K.O., Boyé, M., Croot, P.L., Gervais, F., Gorbunov, M.Y.,  
640 Harrison, P.J., Hiscock, W.T., Laan, P., Lancelot, C., Law, C.S., Lévassieur, M., Marchetti, A., Millero,  
641 F.J., Nishioka, J., Nojiri, Y., van Oijen, T., Riebesell, U., Rijkenberg, M.J.A., Saito, H., Takeda, S.,  
642 Timmermans, K.R., Veldhuis, M.J.W., Waite, A.M., Wong, C.-S., 2005. Synthesis of iron fertilization  
643 experiments: From the Iron Age in the Age of Enlightenment. *J. Geophys. Res. Oceans* 110, C09S16.  
644 doi:10.1029/2004JC002601

645 De Baar, H.J.W., Buma, A.G.J., Nolting, R.F., Cadée, G.C., Jacques, G., Tréguer, P., 1990. On iron limitation of  
646 the Southern Ocean: experimental observations in the Weddell and Scotia Seas. *Mar. Ecol. Prog. Ser.*  
647 65, 105–122. doi:10.3354/meps065105

648 Dilling, L., Alldredge, A.L., 2000. Fragmentation of marine snow by swimming macrozooplankton: A new  
649 process impacting carbon cycling in the sea. *Deep Sea Res. Part Oceanogr. Res. Pap.* 47, 1227–1245.  
650 doi:10.1016/S0967-0637(99)00105-3

651 Dunne, J.P., Sarmiento, J.L., Gnanadesikan, A., 2007. A synthesis of global particle export from the surface  
652 ocean and cycling through the ocean interior and on the seafloor. *Glob. Biogeochem. Cycles* 21,  
653 GB4006. doi:10.1029/2006GB002907

654 Ebersbach, F., Trull, T.W., 2008. Sinking particle properties from polyacrylamide gels during the Kerguelen  
655 Ocean and Plateau compared Study (KEOPS): Zooplankton control of carbon export in an area of

656 persistent natural iron inputs in the Southern Ocean. *Limnol. Oceanogr.* 53, 212–224.  
657 doi:10.4319/lo.2008.53.1.0212

658 Ebersbach, F., Trull, T.W., Davies, D.M., Bray, S.G., 2011. Controls on mesopelagic particle fluxes in the Sub-  
659 Antarctic and Polar Frontal Zones in the Southern Ocean south of Australia in summer—Perspectives  
660 from free-drifting sediment traps. *Deep Sea Res. Part II Top. Stud. Oceanogr.* 58, 2260–2276.  
661 doi:10.1016/j.dsr2.2011.05.025

662 Fischer, G., Ratmeyer, V., Wefer, G., 2000. Organic carbon fluxes in the Atlantic and the Southern Ocean:  
663 relationship to primary production compiled from satellite radiometer data. *Deep Sea Res. Part II Top.*  
664 *Stud. Oceanogr.* 47, 1961–1997. doi:10.1016/S0967-0645(00)00013-8

665 Francois, R., Honjo, S., Krishfield, R., Manganini, S., 2002. Factors controlling the flux of organic carbon to the  
666 bathypelagic zone of the ocean. *Glob. Biogeochem. Cycles* 16, 1087. doi:10.1029/2001GB001722

667 Gall, M.P., Strzepak, R., Maldonado, M., Boyd, P.W., 2001. Phytoplankton processes. Part 2: Rates of primary  
668 production and factors controlling algal growth during the Southern Ocean Iron RElease Experiment  
669 (SOIREE). *Deep Sea Res. Part II Top. Stud. Oceanogr., The Southern Ocean Iron Release Experiment*  
670 (SOIREE) 48, 2571–2590. doi:10.1016/S0967-0645(01)00009-1

671 Gehlen, M., Bopp, L., Emprin, N., Aumont, O., Heinze, C., Ragueneau, O., 2006. Reconciling surface ocean  
672 productivity, export fluxes and sediment composition in a global biogeochemical ocean model.  
673 *Biogeosciences* 3, 521–537. doi:10.5194/bg-3-521-2006

674 Gerber, R.P., Gerber, M.B., 1979. Ingestion of natural particulate organic matter and subsequent assimilation,  
675 respiration and growth by tropical lagoon zooplankton. *Mar. Biol.* 52, 33–43. doi:10.1007/BF00386855

676 Giering, S.L.C., Sanders, R., Lampitt, R.S., Anderson, T.R., Tamburini, C., Boutrif, M., Zubkov, M.V., Marsay,  
677 C.M., Henson, S.A., Saw, K., Cook, K., Mayor, D.J., 2014. Reconciliation of the carbon budget in the  
678 ocean’s twilight zone. *Nature* 507, 480–483. doi:10.1038/nature13123

679 Gilman, D.L., Fuglister, F.J., Mitchell, J.M., 1963. On the Power Spectrum of “Red Noise.” *J. Atmospheric Sci.*  
680 20, 182–184. doi:10.1175/1520-0469(1963)020<0182:OTPSON>2.0.CO;2

681 Gordon, H.R., McCluney, W.R., 1975. Estimation of the depth of sunlight penetration in the sea for remote  
682 sensing. *Appl. Opt.* 14, 413–416.

683 Gruber, N., Gloor, M., Mikaloff Fletcher, S.E., Doney, S.C., Dutkiewicz, S., Follows, M.J., Gerber, M.,  
684 Jacobson, A.R., Joos, F., Lindsay, K., Menemenlis, D., Mouchet, A., Müller, S.A., Sarmiento, J.L.,  
685 Takahashi, T., 2009. Oceanic sources, sinks, and transport of atmospheric CO<sub>2</sub>. *Glob. Biogeochem.*  
686 *Cycles* 23, GB1005. doi:10.1029/2008GB003349

687 Guidi, L., Jackson, G.A., Stemann, L., Miquel, J.C., Picheral, M., Gorsky, G., 2008. Relationship between  
688 particle size distribution and flux in the mesopelagic zone. *Deep Sea Res. Part Oceanogr. Res. Pap.* 55,  
689 1364–1374. doi:10.1016/j.dsr.2008.05.014

690 Gustafsson, O., Andersson, P., Roos, P., Kukulska, Z., Broman, D., Larsson, U., Hajdu, S., Ingri, J., 2004.  
691 Evaluation of the collection efficiency of upper ocean sub-photoc-layer sediment traps: A 24-month in  
692 situ calibration in the open Baltic Sea using 234Th. *Limnol. Oceanogr. Methods* 2, 62–74.  
693 doi:10.4319/lom.2004.2.62

694 Hawley, N., 1988. Flow in Cylindrical Sediment Traps. *J. Gt. Lakes Res.* 14, 76–88. doi:10.1016/S0380-  
695 1330(88)71534-8

696 Henson, S.A., Sanders, R., Madsen, E., 2012. Global patterns in efficiency of particulate organic carbon export  
697 and transfer to the deep ocean. *Glob. Biogeochem. Cycles* 26, GB1028. doi:10.1029/2011GB004099

698 Henson, S.A., Sanders, R., Madsen, E., Morris, P.J., Le Moigne, F., Quartly, G.D., 2011. A reduced estimate of  
699 the strength of the ocean’s biological carbon pump. *Geophys. Res. Lett.* 38, L04606.  
700 doi:10.1029/2011GL046735

701 Henson, S.A., Yool, A., Sanders, R., 2014. Variability in efficiency of particulate organic carbon export: A  
702 model study. *Glob. Biogeochem. Cycles* 29, GB4965. doi:10.1002/2014GB004965

703 Hiscock, W.T., Millero, F.J., 2005. Nutrient and carbon parameters during the Southern Ocean iron experiment  
704 (SOFeX). *Deep Sea Res. Part Oceanogr. Res. Pap.* 52, 2086–2108. doi:10.1016/j.dsr.2005.06.010

705 Honjo, S., Francois, R., Manganini, S., Dymond, J., Collier, R., 2000. Particle fluxes to the interior of the  
706 Southern Ocean in the Western Pacific sector along 170°W. *Deep Sea Res. Part II Top. Stud. Oceanogr.*  
707 47, 3521–3548. doi:10.1016/S0967-0645(00)00077-1

708 Honjo, S., Manganini, S.J., Krishfield, R.A., Francois, R., 2008. Particulate organic carbon fluxes to the ocean  
709 interior and factors controlling the biological pump: A synthesis of global sediment trap programs since  
710 1983. *Prog. Oceanogr.* 76, 217–285. doi:10.1016/j.pocean.2007.11.003

711 Hudson, J.M., Steinberg, D.K., Sutton, T.T., Graves, J.E., Latour, R.J., 2014. Myctophid feeding ecology and  
712 carbon transport along the northern Mid-Atlantic Ridge. *Deep Sea Res. Part Oceanogr. Res. Pap.* 93,  
713 104–116. doi:10.1016/j.dsr.2014.07.002

714 Jacquet, S.H.M., Dehairs, F., Savoye, N., Obernosterer, I., Christaki, U., Monnin, C., Cardinal, D., 2008.  
715 Mesopelagic organic carbon remineralization in the Kerguelen Plateau region tracked by biogenic

716 particulate Ba. *Deep Sea Res. Part II Top. Stud. Oceanogr.* 55, 868–879.  
717 doi:10.1016/j.dsr2.2007.12.038

718 JGOFS Sediment Trap Methods, 1994, in: *Protocols for the Joint Global Ocean Flux Study (JGOFS) Core*  
719 *Measurements. Intergovernmental Oceanographic Commission, Scientific Committee on Oceanic*  
720 *Research Manual and Guides, UNESCO, pp. 157–164.*

721 Jouandet, M.P., Blain, S., Metzl, N., Brunet, C., Trull, T.W., Obernosterer, I., 2008. A seasonal carbon budget  
722 for a naturally iron-fertilized bloom over the Kerguelen Plateau in the Southern Ocean. *Deep Sea Res.*  
723 *Part II Top. Stud. Oceanogr., KEOPS: Kerguelen Ocean and Plateau compared Study 55, 856–867.*  
724 doi:10.1016/j.dsr2.2007.12.037

725 Jouandet, M.-P., Jackson, G.A., Carlotti, F., Picheral, M., Stemmann, L., Blain, S., 2014. Rapid formation of  
726 large aggregates during the spring bloom of Kerguelen Island: observations and model comparisons.  
727 *Biogeosciences* 11, 4393–4406. doi:10.5194/bg-11-4393-2014

728 Jouandet, M.-P., Trull, T.W., Guidi, L., Picheral, M., Ebersbach, F., Stemmann, L., Blain, S., 2011. Optical  
729 imaging of mesopelagic particles indicates deep carbon flux beneath a natural iron-fertilized bloom in  
730 the Southern Ocean. *Limnol. Oceanogr.* 56, 1130–1140. doi:10.4319/lo.2011.56.3.1130

731 Karleskind, P., Lévy, M., Memery, L., 2011. Subduction of carbon, nitrogen, and oxygen in the northeast  
732 Atlantic. *J. Geophys. Res. Oceans* 116, C02025. doi:10.1029/2010JC006446

733 Kohfeld, K.E., Quéré, C.L., Harrison, S.P., Anderson, R.F., 2005. Role of Marine Biology in Glacial-Interglacial  
734 CO<sub>2</sub> Cycles. *Science* 308, 74–78. doi:10.1126/science.1105375

735 Korb, R.E., Whitehouse, M., 2004. Contrasting primary production regimes around South Georgia, Southern  
736 Ocean: large blooms versus high nutrient, low chlorophyll waters. *Deep Sea Res. Part Oceanogr. Res.*  
737 *Pap.* 51, 721–738. doi:10.1016/j.dsr.2004.02.006

738 Koubbi, P., Duhamel, G., Hebert, C., 2001. Seasonal relative abundance of fish larvae inshore at Îles Kerguelen,  
739 Southern Ocean. *Antarct. Sci.* 13, 385–392. doi:10.1017/S0954102001000542

740 Koubbi, P., Ibanez, F., Duhamel, G., 1991. Environmental influences on spatio-temporal oceanic distribution of  
741 ichthyoplankton around the Kerguelen Islands (Southern Ocean). *Mar. Ecol. Prog. Ser.* 72, 225–238.

742 Lampitt, R.S., Antia, A.N., 1997. Particle flux in deep seas: regional characteristics and temporal variability.  
743 *Deep Sea Res. Part Oceanogr. Res. Pap.* 44, 1377–1403. doi:10.1016/S0967-0637(97)00020-4

744 Lampitt, R.S., Boorman, B., Brown, L., Lucas, M., Salter, I., Sanders, R., Saw, K., Seeyave, S., Thomalla, S.J.,  
745 Turnewitsch, R., 2008. Particle export from the euphotic zone: Estimates using a novel drifting  
746 sediment trap, 234Th and new production. *Deep Sea Res. Part Oceanogr. Res. Pap.* 55, 1484–1502.  
747 doi:10.1016/j.dsr.2008.07.002

748 Lam, P.J., Bishop, J.K.B., 2007. High biomass, low export regimes in the Southern Ocean. *Deep Sea Res. Part II*  
749 *Top. Stud. Oceanogr.* 54, 601–638. doi:10.1016/j.dsr2.2007.01.013

750 Lam, P.J., Doney, S.C., Bishop, J.K.B., 2011. The dynamic ocean biological pump: Insights from a global  
751 compilation of particulate organic carbon, CaCO<sub>3</sub>, and opal concentration profiles from the  
752 mesopelagic. *Glob. Biogeochem. Cycles* 25, GB3009. doi:10.1029/2010GB003868

753 Landry, M.R., Constantinou, J., Latasa, M., Brown, S.L., Bidigare, R.R., Ondrusek, M.E., 2000. Biological  
754 response to iron fertilization in the eastern equatorial Pacific (IronEx II). III. Dynamics of  
755 phytoplankton growth and microzooplankton grazing. *Mar. Ecol. Prog. Ser.* 201, 57–72.  
756 doi:10.3354/meps201057

757 Laurenceau-Cornec, E.C., Trull, T.W., Davies, D.M., Bray, S.G., Doran, J., Planchon, F., Carlotti, F., Jouandet,  
758 M.-P., Cavagna, A.-J., Waite, A.M., Blain, S., 2015. The relative importance of phytoplankton  
759 aggregates and zooplankton fecal pellets to carbon export: insights from free-drifting sediment trap  
760 deployments in naturally iron-fertilised waters near the Kerguelen Plateau. *Biogeosciences* 12, 1007–  
761 1027. doi:10.5194/bg-12-1007-2015

762 Laws, E.A., D'Sa, E., Naik, P., 2011. Simple equations to estimate ratios of new or export production to total  
763 production from satellite-derived estimates of sea surface temperature and primary production. *Limnol.*  
764 *Oceanogr. Methods* 593–601. doi:10.4319/lom.2011.9.593

765 Laws, E.A., Falkowski, P.G., Smith, W.O., Ducklow, H., McCarthy, J.J., 2000. Temperature effects on export  
766 production in the open ocean. *Glob. Biogeochem. Cycles* 14, 1231–1246. doi:10.1029/1999GB001229

767 Lefèvre, D., Guigue, C., Obernosterer, I., 2008. The metabolic balance at two contrasting sites in the Southern  
768 Ocean: The iron-fertilized Kerguelen area and HNLC waters. *Deep Sea Res. Part II Top. Stud.*  
769 *Oceanogr., KEOPS: Kerguelen Ocean and Plateau compared Study 55, 766–776.*  
770 doi:10.1016/j.dsr2.2007.12.006

771 Le Moigne, F.A.C., Sanders, R.J., Villa-Alfageme, M., Martin, A.P., Pabortsava, K., Planquette, H., Morris, P.J.,  
772 Thomalla, S.J., 2012. On the proportion of ballast versus non-ballast associated carbon export in the  
773 surface ocean. *Geophys. Res. Lett.* 39, L15610. doi:10.1029/2012GL052980

774 Lenton, A., Tilbrook, B., Law, R.M., Bakker, D., Doney, S.C., Gruber, N., Ishii, M., Hoppema, M., Lovenduski,  
775 N.S., Matear, R.J., McNeil, B.I., Metzl, N., Mikaloff Fletcher, S.E., Monteiro, P.M.S., Rödenbeck, C.,

776 Sweeney, C., Takahashi, T., 2013. Sea–air CO<sub>2</sub> fluxes in the Southern Ocean for the period 1990–2009.  
777 *Biogeosciences* 10, 4037–4054. doi:10.5194/bg-10-4037-2013

778 Le Quéré, C., Andres, R.J., Boden, T., Conway, T., Houghton, R.A., House, J.I., Marland, G., Peters, G.P., van  
779 der Werf, G.R., Ahlström, A., Andrew, R.M., Bopp, L., Canadell, J.G., Ciais, P., Doney, S.C., Enright,  
780 C., Friedlingstein, P., Huntingford, C., Jain, A.K., Jourdain, C., Kato, E., Keeling, R.F., Klein  
781 Goldewijk, K., Levis, S., Levy, P., Lomas, M., Poulter, B., Raupach, M.R., Schwinger, J., Sitch, S.,  
782 Stocker, B.D., Viovy, N., Zaehle, S., Zeng, N., 2013. The global carbon budget 1959–2011. *Earth Syst.*  
783 *Sci. Data* 5, 165–185. doi:10.5194/essd-5-165-2013

784 Levy, M., Bopp, L., Karleskind, P., Resplandy, L., Ethe, C., Pinsard, F., 2013. Physical pathways for carbon  
785 transfers between the surface mixed layer and the ocean interior. *Glob. Biogeochem. Cycles* 27, 1001–  
786 1012. doi:10.1002/gbc.20092

787 Lima, I.D., Lam, P.J., Doney, S.C., 2014. Dynamics of particulate organic carbon flux in a global ocean model.  
788 *Biogeosciences* 11, 1177–1198. doi:10.5194/bg-11-1177-2014

789 Lutz, M.J., Caldeira, K., Dunbar, R.B., Behrenfeld, M.J., 2007. Seasonal rhythms of net primary production and  
790 particulate organic carbon flux to depth describe the efficiency of biological pump in the global ocean.  
791 *J. Geophys. Res. Oceans* 112, C10011. doi:10.1029/2006JC003706

792 Maiti, K., Charette, M.A., Buesseler, K.O., Kahru, M., 2013. An inverse relationship between production and  
793 export efficiency in the Southern Ocean. *Geophys. Res. Lett.* 40, 1557–1561. doi:10.1002/grl.50219

794 Manno, C., Stowasser, G., Enderlein, P., Fielding, S., Tarling, G.A., 2014. The contribution of zooplankton  
795 faecal pellets to deep carbon transport in the Scotia Sea (Southern Ocean). *Biogeosciences Discuss* 11,  
796 16105–16134. doi:10.5194/bgd-11-16105-2014

797 Maraldi, C., Lyard, F., Testut, L., Coleman, R., 2011. Energetics of internal tides around the Kerguelen Plateau  
798 from modeling and altimetry. *J. Geophys. Res. Oceans* 116, C06004. doi:10.1029/2010JC006515

799 Maraldi, C., Mongin, M., Coleman, R., Testut, L., 2009. The influence of lateral mixing on a phytoplankton  
800 bloom: Distribution in the Kerguelen Plateau region. *Deep Sea Res. Part Oceanogr. Res. Pap.* 56, 963–  
801 973. doi:10.1016/j.dsr.2008.12.018

802 Maritorea, S., Siegel, D.A., 2005. Consistent merging of satellite ocean color data sets using a bio-optical  
803 model. *Remote Sens. Environ.* 94, 429–440. doi:10.1016/j.rse.2004.08.014

804 Martin, J.H., Knauer, G.A., Karl, D.M., Broenkow, W.W., 1987. VERTEX: carbon cycling in the northeast  
805 Pacific. *Deep Sea Res. Part Oceanogr. Res. Pap.* 34, 267–285. doi:10.1016/0198-0149(87)90086-0

806 Martin, P., van der Loeff, M.R., Cassar, N., Vandromme, P., d' Ovidio, F., Stemmann, L., Rengarajan, R.,  
807 Soares, M., González, H.E., Ebersbach, F., Lampitt, R.S., Sanders, R., Barnett, B.A., Smetacek, V.,  
808 Naqvi, S.W.A., 2013. Iron fertilization enhanced net community production but not downward particle  
809 flux during the Southern Ocean iron fertilization experiment LOHAFEX. *Glob. Biogeochem. Cycles*  
810 27, 871–881. doi:10.1002/gbc.20077

811 Matsuno, K., Yamaguchi, A., Fujiwara, A., Onodera, J., Watanabe, E., Imai, I., Chiba, S., Harada, N., Kikuchi,  
812 T., 2014. Seasonal changes in mesozooplankton swimmers collected by sediment trap moored at a  
813 single station on the Northwind Abyssal Plain in the western Arctic Ocean. *J. Plankton Res.* 36, 490–  
814 502. doi:10.1093/plankt/fbt092

815 Measures, C.I., Brown, M.T., Selph, K.E., Apprill, A., Zhou, M., Hatta, M., Hiscock, W.T., 2013. The influence  
816 of shelf processes in delivering dissolved iron to the HNLC waters of the Drake Passage, Antarctica.  
817 *Deep Sea Res. Part II Top. Stud. Oceanogr.* 90, 77–88. doi:10.1016/j.dsr2.2012.11.004

818 Metzl, N., Brunet, C., Jabaud-Jan, A., Poisson, A., Schauer, B., 2006. Summer and winter air–sea CO<sub>2</sub> fluxes in  
819 the Southern Ocean. *Deep Sea Res. Part Oceanogr. Res. Pap.* 53, 1548–1563.  
820 doi:10.1016/j.dsr.2006.07.006

821 Moore, J.K., Doney, S.C., Lindsay, K., 2004. Upper ocean ecosystem dynamics and iron cycling in a global  
822 three-dimensional model. *Glob. Biogeochem. Cycles* 18, GB4028. doi:10.1029/2004GB002220

823 Morales, C.E., 1987. Carbon and nitrogen content of copepod faecal pellets: effect of food concentration and  
824 feeding behaviour. *Mar. Ecol. Prog. Ser.* 36, 107–114.

825 Obernosterer, I., Christaki, U., Lefèvre, D., Catala, P., Van Wambeke, F., Lebaron, P., 2008. Rapid bacterial  
826 mineralization of organic carbon produced during a phytoplankton bloom induced by natural iron  
827 fertilization in the Southern Ocean. *Deep Sea Res. Part II Top. Stud. Oceanogr.* 55, 777–789.  
828 doi:10.1016/j.dsr2.2007.12.005

829 O'Neill, L.P., Benitez-Nelson, C.R., Styles, R.M., Tappa, E., Thunell, R.C., 2005. Diagenetic effects on  
830 particulate phosphorus samples collected using formalin poisoned sediment traps. *Limnol. Oceanogr.*  
831 *Methods* 3, 308–317. doi:10.4319/lom.2005.3.308

832 Park, Y.-H., Charriaud, E., Pino, D.R., Jeandel, C., 1998. Seasonal and interannual variability of the mixed layer  
833 properties and steric height at station KERFIX, southwest of Kerguelen. *J. Mar. Syst.* 17, 571–586.  
834 doi:10.1016/S0924-7963(98)00065-7

835 Park, Y.-H., Fuda, J.-L., Durand, I., Naveira Garabato, A.C., 2008a. Internal tides and vertical mixing over the  
836 Kerguelen Plateau. *Deep Sea Res. Part II Top. Stud. Oceanogr.* 55, 582–593.  
837 doi:10.1016/j.dsr2.2007.12.027

838 Park, Y.-H., Roquet, F., Durand, I., Fuda, J.-L., 2008b. Large-scale circulation over and around the Northern  
839 Kerguelen Plateau. *Deep Sea Res. Part II Top. Stud. Oceanogr.* 55, 566–581.  
840 doi:10.1016/j.dsr2.2007.12.030

841 Peterson, M.L., Wakeham, S.G., Lee, C., Askea, M.A., Miquel, J.C., 2005. Novel techniques for collection of  
842 sinking particles in the ocean and determining their settling rates. *Limnol. Oceanogr. Methods* 3, 520–  
843 532. doi:10.4319/lom.2005.3.520

844 Picheral, M., Guidi, L., Stemann, L., Karl, D.M., Iddaoud, G., Gorsky, G., 2010. The Underwater Vision  
845 Profiler 5: An advanced instrument for high spatial resolution studies of particle size spectra and  
846 zooplankton. *Limnol. Oceanogr. Methods* 8, 462–473. doi:10.4319/lom.2010.8.462

847 Planchon, F., Ballas, D., Cavagna, A.-J., Bowie, A.R., Davies, D., Trull, T., Laurenceau, E., Van Der Merwe, P.,  
848 Dehairs, F., 2014. Carbon export in the naturally iron-fertilized Kerguelen area of the Southern Ocean  
849 based on the 234Th approach. *Biogeosciences Discuss* 11, 15991–16032. doi:10.5194/bgd-11-15991-  
850 2014

851 Pollard, R., Sanders, R., Lucas, M., Statham, P., 2007. The Crozet Natural Iron Bloom and Export Experiment  
852 (CROZEX). *Deep Sea Res. Part II Top. Stud. Oceanogr.* 54, 1905–1914.  
853 doi:10.1016/j.dsr2.2007.07.023

854 Pollard, R.T., Salter, I., Sanders, R.J., Lucas, M.I., Moore, C.M., Mills, R.A., Statham, P.J., Allen, J.T., Baker,  
855 A.R., Bakker, D.C.E., Charette, M.A., Fielding, S., Fones, G.R., French, M., Hickman, A.E., Holland,  
856 R.J., Hughes, J.A., Jickells, T.D., Lampitt, R.S., Morris, P.J., Nédélec, F.H., Nielsdóttir, M., Planquette,  
857 H., Popova, E.E., Poulton, A.J., Read, J.F., Seeyave, S., Smith, T., Stinchcombe, M., Taylor, S.,  
858 Thomalla, S., Venables, H.J., Williamson, R., Zubkov, M.V., 2009. Southern Ocean deep-water carbon  
859 export enhanced by natural iron fertilization. *Nature* 457, 577–580. doi:10.1038/nature07716

860 Rembauville, M., Blain, S., Armand, L., Quéguiner, B., Salter, I., 2014. Export fluxes in a naturally fertilized  
861 area of the Southern Ocean, the Kerguelen Plateau: ecological vectors of carbon and biogenic silica to  
862 depth (Part 2). *Biogeosciences Discuss* 11, 17089–17150. doi:10.5194/bgd-11-17089-2014

863 Rigual-Hernández, A.S., Trull, T.W., Bray, S.G., Closset, I., Armand, L.K., 2015. Seasonal dynamics in diatom  
864 and particulate export fluxes to the deep sea in the Australian sector of the southern Antarctic Zone. *J.*  
865 *Mar. Syst.* 142, 62–74. doi:10.1016/j.jmarsys.2014.10.002

866 Rivkin, R.B., Legendre, L., 2001. Biogenic carbon cycling in the upper ocean: effects of microbial respiration.  
867 *Science* 291, 2398–2400. doi:10.1126/science.291.5512.2398

868 Rynearson, T.A., Richardson, K., Lampitt, R.S., Sieracki, M.E., Poulton, A.J., Lyngsgaard, M.M., Perry, M.J.,  
869 2013. Major contribution of diatom resting spores to vertical flux in the sub-polar North Atlantic. *Deep*  
870 *Sea Res. Part Oceanogr. Res. Pap.* 82, 60–71. doi:10.1016/j.dsr.2013.07.013

871 Saba, G.K., Steinberg, D.K., 2012. Abundance, Composition, and Sinking Rates of Fish Fecal Pellets in the  
872 Santa Barbara Channel. *Sci. Rep.* 2. doi:10.1038/srep00716

873 Salter, I., Kemp, A.E.S., Lampitt, R.S., Gledhill, M., 2010. The association between biogenic and inorganic  
874 minerals and the amino acid composition of settling particles. *Limnol. Oceanogr.* 55, 2207–2218.  
875 doi:10.4319/lo.2010.55.5.2207

876 Salter, I., Kemp, A.E.S., Moore, C.M., Lampitt, R.S., Wolff, G.A., Holtvoeth, J., 2012. Diatom resting spore  
877 ecology drives enhanced carbon export from a naturally iron-fertilized bloom in the Southern Ocean.  
878 *Glob. Biogeochem. Cycles* 26, GB1014. doi:10.1029/2010GB003977

879 Salter, I., Lampitt, R.S., Sanders, R., Poulton, A., Kemp, A.E.S., Boorman, B., Saw, K., Pearce, R., 2007.  
880 Estimating carbon, silica and diatom export from a naturally fertilised phytoplankton bloom in the  
881 Southern Ocean using PELAGRA: A novel drifting sediment trap. *Deep Sea Res. Part II Top. Stud.*  
882 *Oceanogr.*, The Crozet Natural Iron Bloom and Export Experiment CROZEX 54, 2233–2259.  
883 doi:10.1016/j.dsr2.2007.06.008

884 Salter, I., Schiebel, R., Ziveri, P., Movellan, A., Lampitt, R., Wolff, G.A., 2014. Carbonate counter pump  
885 stimulated by natural iron fertilization in the Polar Frontal Zone. *Nat. Geosci.* 7, 885–889.  
886 doi:10.1038/ngeo2285

887 Sarmiento, J.L., Gruber, N., 2006. *Ocean Biogeochemical Dynamics*. Princeton University Press, Princeton.

888 Sarmiento, J.L., Le Quééré, C., 1996. Oceanic Carbon Dioxide Uptake in a Model of Century-Scale Global  
889 Warming. *Science* 274, 1346–1350.

890 Sarthou, G., Timmermans, K.R., Blain, S., Tréguer, P., 2005. Growth physiology and fate of diatoms in the  
891 ocean: a review. *J. Sea Res., Iron Resources and Oceanic Nutrients - Advancement of Global*  
892 *Environmental Simulations* 53, 25–42. doi:10.1016/j.seares.2004.01.007

893 Savoye, N., Benitez-Nelson, C., Burd, A.B., Cochran, J.K., Charette, M., Buesseler, K.O., Jackson, G.A., Roy-  
894 Barman, M., Schmidt, S., Elskens, M., 2006.  $^{234}\text{Th}$  sorption and export models in the water column: A  
895 review. *Mar. Chem.* 100, 234–249. doi:10.1016/j.marchem.2005.10.014

896 Savoye, N., Trull, T.W., Jacquet, S.H.M., Navez, J., Dehairs, F., 2008.  $^{234}\text{Th}$ -based export fluxes during a  
897 natural iron fertilization experiment in the Southern Ocean (KEOPS). *Deep Sea Res. Part II Top. Stud.*  
898 *Oceanogr.*, KEOPS: Kerguelen Ocean and Plateau compared Study 55, 841–855.  
899 doi:10.1016/j.dsr2.2007.12.036

900 Schlitzer, R., 2004. Export production in the Equatorial and North Pacific derived from dissolved oxygen,  
901 nutrient and carbon data. *J. Oceanogr.* Vol 60 No 1 Pp 53–62.

902 Schulz, M., Mudelsee, M., 2002. REDFIT: estimating red-noise spectra directly from unevenly spaced  
903 paleoclimatic time series. *Comput. Geosci.* 28, 421–426. doi:10.1016/S0098-3004(01)00044-9

904 Seeyave, S., Lucas, M.I., Moore, C.M., Poulton, A.J., 2007. Phytoplankton productivity and community  
905 structure in the vicinity of the Crozet Plateau during austral summer 2004/2005. *Deep Sea Res. Part II*  
906 *Top. Stud. Oceanogr.*, The Crozet Natural Iron Bloom and Export Experiment CROZEX 54, 2020–  
907 2044. doi:10.1016/j.dsr2.2007.06.010

908 Smetacek, V., Assmy, P., Henjes, J., 2004. The role of grazing in structuring Southern Ocean pelagic ecosystems  
909 and biogeochemical cycles. *Antarct. Sci.* 16, 541–558. doi:10.1017/S0954102004002317

910 Smith, R.C., 1981. Remote sensing and depth distribution of ocean chlorophyll. *Mar. Ecol.-Prog. Ser.* 5, 359–  
911 361.

912 Tarling, G.A., Ward, P., Atkinson, A., Collins, M.A., Murphy, E.J., 2012. DISCOVERY 2010: Spatial and  
913 temporal variability in a dynamic polar ecosystem. *Deep Sea Res. Part II Top. Stud. Oceanogr.* 59–60,  
914 1–13. doi:10.1016/j.dsr2.2011.10.001

915 Thomalla, S.J., Fauchereau, N., Swart, S., Monteiro, P.M.S., 2011. Regional scale characteristics of the seasonal  
916 cycle of chlorophyll in the Southern Ocean. *Biogeosciences* 8, 2849–2866. doi:10.5194/bg-8-2849-  
917 2011

918 Trull, T.W., Bray, S.G., Buesseler, K.O., Lamborg, C.H., Manganini, S., Moy, C., Valdes, J., 2008. In situ  
919 measurement of mesopelagic particle sinking rates and the control of carbon transfer to the ocean  
920 interior during the Vertical Flux in the Global Ocean (VERTIGO) voyages in the North Pacific. *Deep*  
921 *Sea Res. Part II Top. Stud. Oceanogr.* 55, 1684–1695. doi:10.1016/j.dsr2.2008.04.021

922 Trull, T.W., Davies, D., Casciotti, K., 2008. Insights into nutrient assimilation and export in naturally iron-  
923 fertilized waters of the Southern Ocean from nitrogen, carbon and oxygen isotopes. *Deep Sea Res. Part*  
924 *II Top. Stud. Oceanogr.* 55, 820–840. doi:10.1016/j.dsr2.2007.12.035

925 Tsuda, A., Takeda, S., Saito, H., Nishioka, J., Kudo, I., Nojiri, Y., Suzuki, K., Uematsu, M., Wells, M.L.,  
926 Tsumune, D., Yoshimura, T., Aono, T., Aramaki, T., Cochlan, W.P., Hayakawa, M., Imai, K., Isada, T.,  
927 Iwamoto, Y., Johnson, W.K., Kameyama, S., Kato, S., Kiyosawa, H., Kondo, Y., Levasseur, M.,  
928 Machida, R.J., Nagao, I., Nakagawa, F., Nakanishi, T., Nakatsuka, S., Narita, A., Noiri, Y., Obata, H.,  
929 Ogawa, H., Oguma, K., Ono, T., Sakuragi, T., Sasakawa, M., Sato, M., Shimamoto, A., Takata, H.,  
930 Trick, C.G., Watanabe, Y.W., Wong, C.S., Yoshie, N., 2007. Evidence for the grazing hypothesis:  
931 Grazing reduces phytoplankton responses of the HNLC ecosystem to iron enrichment in the western  
932 subarctic pacific (SEEDS II). *J. Oceanogr.* 63, 983–994. doi:10.1007/s10872-007-0082-x

933 Uitz, J., Claustre, H., Griffiths, F.B., Ras, J., Garcia, N., Sandroni, V., 2009. A phytoplankton class-specific  
934 primary production model applied to the Kerguelen Islands region (Southern Ocean). *Deep Sea Res.*  
935 *Part Oceanogr. Res. Pap.* 56, 541–560. doi:10.1016/j.dsr.2008.11.006

936 Villareal, T.A., Adornato, L., Wilson, C., Schoenbaechler, C.A., 2011. Summer blooms of diatom-diazotroph  
937 assemblages and surface chlorophyll in the North Pacific gyre: A disconnect. *J. Geophys. Res. Oceans*  
938 116, C03001. doi:10.1029/2010JC006268

939 Volk, T., Hoffert, M.I., 1985. Ocean carbon pumps: Analysis of relative strengths and efficiencies in ocean-  
940 driven atmospheric CO<sub>2</sub> changes, in: Sundquist, E.T., Broecker, W.S. (Eds.), *Geophysical Monograph*  
941 *Series.* American Geophysical Union, Washington, D. C., pp. 99–110.

942

943 **Table 1:** Dynamics of carbon and nitrogen export fluxes at station A3 collected by the  
 944 sediment trap at 289 m.

Cup	Start	Stop	Fluxes ( $\text{mmol m}^{-2} \text{d}^{-1}$ )			Contribution to annual export (%)	
			POC	PON	POC:PON	POC	PON
1	21/10/2011	04/11/2011	0.15±0.01	0.02±0.00	6.80±0.56	2.11±0.06	2.30±0.01
2	04/11/2011	18/11/2011	0.14 ±0.01	0.02±0.00	6.09±0.67	1.94±0.16	2.27±0.15
3	18/11/2011	02/12/2011	0.15±0.01	0.02±0.00	7.33±0.31	2.12±0.06	1.99±0.06
4	02/12/2011	12/12/2011	1.60±0.04	0.23±0.01	6.95±0.29	16.18±0.45	16.48±0.07
5	12/12/2011	22/12/2011	0.34±0.00	0.05±0.00	6.87±0.08	3.41±0.03	3.64±0.03
6	22/12/2011	01/01/2012	0.51±0.04	0.08±0.01	6.70±0.78	4.82±0.76	5.50±0.39
7	01/01/2012	11/01/2012	0.42±0.02	0.06±0.00	6.73±0.46	4.23±0.14	4.65±0.42
8	11/01/2012	25/01/2012	0.34±0.01	0.05±0.00	6.94±0.38	4.83±0.18	4.84±0.11
9	25/01/2012	08/02/2012	1.47±0.03	0.20±0.01	7.38±0.26	20.98±0.57	21.07±0.05
10	08/02/2012	22/02/2012	0.55±0.04	0.08±0.00	6.97±0.88	7.83±0.64	8.36±0.57
11	22/02/2012	31/05/2012	0.27±0.01	0.03±0.00	8.09±0.22	26.84±0.47	24.12±0.20
12	31/05/2012	07/09/2012	0.04±0.00	0.01±0.00	6.06±0.17	4.71±0.90	4.78±0.09
<b>Annual export (<math>\text{mmol m}^{-2} \text{y}^{-1}</math>)</b>			98.24±4.35	13.59±0.30			

945

946

947 **Table 2:** Number of swimmer individuals found in each cup and swimmer intrusion rate  
 948 (number d<sup>-1</sup>, *bold italic* numbers) for each taxa and for the total swimmers.

Cup	Copepod	Pteropod	Euphausi d	Ostracod	Amphipo d	Cnidaria n	Polychaet e	Ctenopho re	Siphonop hore	Salp	Total
1	166	13	1	2	1	0	0	0	0	0	183
	<i>12</i>	<i>1</i>	<i>&lt;1</i>	<i>&lt;1</i>	<i>&lt;1</i>	<i>0</i>	<i>0</i>	<i>0</i>	<i>0</i>	<i>0</i>	<i>13</i>
2	55	0	0	0	0	0	0	0	0	0	55
	<i>4</i>	<i>0</i>	<i>0</i>	<i>0</i>	<i>0</i>	<i>0</i>	<i>0</i>	<i>0</i>	<i>0</i>	<i>0</i>	<i>4</i>
3	0	0	0	0	0	0	0	0	0	0	0
	<i>0</i>	<i>0</i>	<i>0</i>	<i>0</i>	<i>0</i>	<i>0</i>	<i>0</i>	<i>0</i>	<i>0</i>	<i>0</i>	<i>0</i>
4	113	0	0	0	0	0	0	0	0	0	113
	<i>11</i>	<i>0</i>	<i>0</i>	<i>0</i>	<i>0</i>	<i>0</i>	<i>0</i>	<i>0</i>	<i>0</i>	<i>0</i>	<i>11</i>
5	0	0	0	0	0	0	0	0	0	0	0
	<i>0</i>	<i>0</i>	<i>0</i>	<i>0</i>	<i>0</i>	<i>0</i>	<i>0</i>	<i>0</i>	<i>0</i>	<i>0</i>	<i>0</i>
6	540	0	1	0	2	5	1	4	1	0	554
	<i>54</i>	<i>0</i>	<i>&lt;1</i>	<i>0</i>	<i>&lt;1</i>	<i>&lt;1</i>	<i>0</i>	<i>0</i>	<i>0</i>	<i>0</i>	<i>55</i>
7	583	0	0	0	0	2	2	3	0	0	590
	<i>58</i>	<i>0</i>	<i>0</i>	<i>0</i>	<i>0</i>	<i>&lt;1</i>	<i>&lt;1</i>	<i>&lt;1</i>	<i>0</i>	<i>0</i>	<i>58</i>
8	686	33	2	2	8	5	1	4	0	0	741
	<i>49</i>	<i>2</i>	<i>&lt;1</i>	<i>&lt;1</i>	<i>1</i>	<i>&lt;1</i>	<i>&lt;1</i>	<i>&lt;1</i>	<i>0</i>	<i>0</i>	<i>52</i>
9	392	14	4	3	121	4	2	0	0	0	540
	<i>28</i>	<i>1</i>	<i>&lt;1</i>	<i>&lt;1</i>	<i>9</i>	<i>&lt;1</i>	<i>&lt;1</i>	<i>0</i>	<i>0</i>	<i>0</i>	<i>38</i>
10	264	69	1	2	18	11	0	2	0	0	367
	<i>19</i>	<i>5</i>	<i>&lt;1</i>	<i>&lt;1</i>	<i>1</i>	<i>1</i>	<i>0</i>	<i>&lt;1</i>	<i>0</i>	<i>0</i>	<i>26</i>
11	54	0	0	0	29	4	1	0	0	0	88
	<i>1</i>	<i>0</i>	<i>0</i>	<i>0</i>	<i>&lt;1</i>	<i>&lt;1</i>	<i>&lt;1</i>	<i>0</i>	<i>0</i>	<i>0</i>	<i>1</i>
12	1481	44	5	7	2	3	2	0	0	1	1544
	<i>15</i>	<i>&lt;1</i>	<i>&lt;1</i>	<i>&lt;1</i>	<i>&lt;1</i>	<i>&lt;1</i>	<i>&lt;1</i>	<i>0</i>	<i>0</i>	<i>&lt;1</i>	<i>15</i>

949

950



951 **Table 3:** Synthesis of estimates of POC fluxes at the base of, or under, the mixed layer at  
 952 station A3 from the KEOPS 1 cruise.

Author	Method	Period	Depth (m)	POC flux ( $\text{mmol m}^{-2} \text{d}^{-1}$ )	
<b>KEOPS1</b>					
Savoie et al., 2008	$^{234}\text{Th}$ deficit	23 Jan – 12 Feb 2005	100	$23 \pm 3.6$	
			150	$25.7 \pm 3.6$	
			200	$24.5 \pm 6.8$	
Ebersbach and Trull, 2008	Drifting gel trap, optical measurements and constant C conversion factor	4 Feb 2005	200	23.9	
			100	5.3	
		12 Feb 2005	200	5.2	
			330	0.7	
			430	1	
Jouandet et al., 2008	Annual DIC budget	Annual	MLD base	85	
Trull et al., 2008b	Drifting sediment trap	4 Feb 2005	200	7.3-10	
		12 Feb 2005		3-3.1	
Jouandet et al., 2011	In situ optical measurement (UVP) and power function C conversion factor	22 Jan 2005	200	72.4	
			330	27.2	
			400	21.6	
		23 Jan 2005	200	29.8	
			330	26.8	
			400	15.9	
		12 Feb 2005	200	4.8	
			330	5.6	
			400	7.9	
<b>KEOPS2</b>					
Planchon et al., 2014	$^{234}\text{Th}$ deficit, steady state model	20 Oct 2011	100	$3.5 \pm 0.9$	
			150	$3.9 \pm 0.9$	
		16 Nov 2011	200	$3.7 \pm 0.9$	
			100	$4.6 \pm 1.5$	
		$^{234}\text{Th}$ deficit, non steady state model	16 Nov 2011	150	$7.1 \pm 1.5$
				200	$3.1 \pm 0.6$
			100	100	$7.3 \pm 1.8$
				150	$8.4 \pm 1.8$
	200	$3.8 \pm 0.8$			
Laurenceau-Cornec et al., 2015	Drifting gel trap, optical measurement of particles	16 Nov 2011	210	5.5	
			210	2.2	
Jouandet et al., 2014	In situ optical measurement (UVP) and power function C conversion factor	21 Oct 2011	200	0.2	
			350	0.1	
		16 Nov 2011	200	1.9	
			350	0.3	



954 **Figures captions**

955 **Figure 1.** Localization of the Kerguelen Plateau in the Indian sector of the Southern Ocean  
956 and detailed map of the satellite-derived surface chlorophyll *a* concentration (MODIS level 3  
957 product) averaged over the sediment trap deployment period. Sediment trap location at the A3  
958 station is represented by a black dot, whereas the black circle represents the 100 km radius  
959 area used to average the surface chlorophyll *a* time series. Arrows represent surface  
960 geostrophic circulation derived from the absolute dynamic topography (AVISO product).  
961 Positions of the Antarctic Circumpolar Current core (AAC core), the Polar Front (PF) and the  
962 Fawn Through Current (FTC) are shown by thick black arrows. Grey lines are 500 m and  
963 1000 m isobaths.

964 **Figure 2.** Schematic of the instrumented mooring line against vertical temperature profiles.  
965 The sediment trap and the current meter/CTD sensor location on the mooring line are shown  
966 by white circles. Temperature profiles performed during the sediment trap deployment (20  
967 October 2011) are represented by grey lines. Black full line is the median temperature profile  
968 from 12 casts realized on the 16 November 2011. Dashed black lines are the first and third  
969 quartiles from these casts. The grey rectangle represents the Kerguelen Plateau seafloor. The  
970 different water masses are Antarctic Surface Water (AASW), Winter Water (WW) and Upper  
971 Circumpolar Deep Water (UCDW).

972 **Figure 3.** Hydrological properties recorded by the instrument mooring at station A3. a) depth  
973 of the CTD sensor, b) salinity, c) potential temperature, d) line angle, e) current speed, grey  
974 lines are raw data, black lines are low-pass filtered data with a Gaussian filter (40 hour  
975 window as suggested by the spectral analysis), f) direction and speed of currents represented  
976 by vectors (under sampled with a 5 hours interval) and g) wind rose plot of current direction

977 and intensities, dotted circles are directions relative frequencies and colors refer to current  
978 speed ( $\text{m s}^{-1}$ ).

979 **Figure 4.** Potential temperature/salinity diagram at station A3. Data are from the moored  
980 CTD (black dots), KEOPS1 (blue line) and KEOPS2 (red line). Grey lines are potential  
981 density anomaly. The different water masses are Antarctic Surface Water (AASW), Winter  
982 Water (WW) and Upper Circumpolar Deep Water (UCDW).

983

984 **Figure 5.** Power spectrum of the spectral analysis of a) depth time series and b) potential  
985 density anomaly time series. Pure red noise (null hypothesis) is represented by red dashed  
986 lines for each variable. The period corresponding to a significant power peak (power peak  
987 higher than the red noise) is written.

988 **Figure 6.** Progressive vector diagram (integration of the current vectors all along the current  
989 meter record) calculated from current meter data at 319 m. The color scale refers to date.

990 **Figure 7.** Seasonal variations of surface chlorophyll *a* and particulate organic carbon (POC)  
991 export. a) Seasonal surface chlorophyll concentration and 16 years climatology (Globcolour)  
992 averaged in a 100 km radius around the station A3 station The black line represents the  
993 climatology calculated for the period 1997/2013, whilst the green line corresponds to the  
994 sediment trap deployment period (2011/2012). b) POC flux (grey bars) and mass percentage  
995 of POC (red dotted line). Error bars are standard deviations from triplicates, bold italic  
996 numbers refer to cup number.

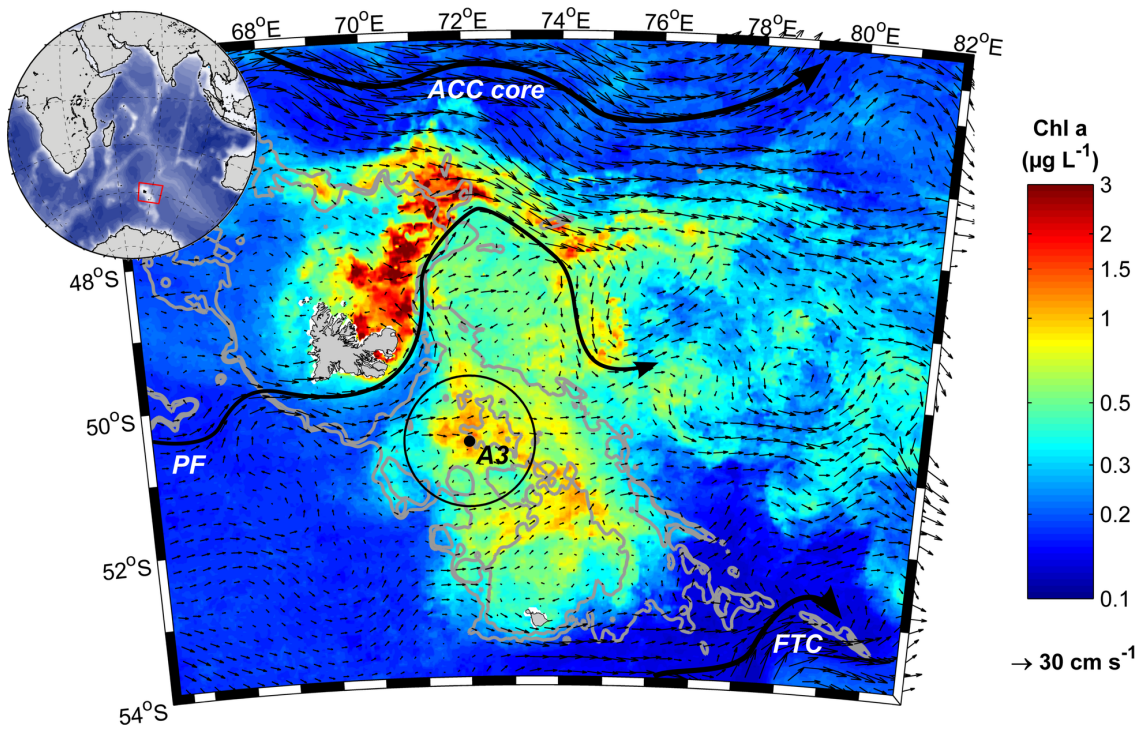


Figure 1.

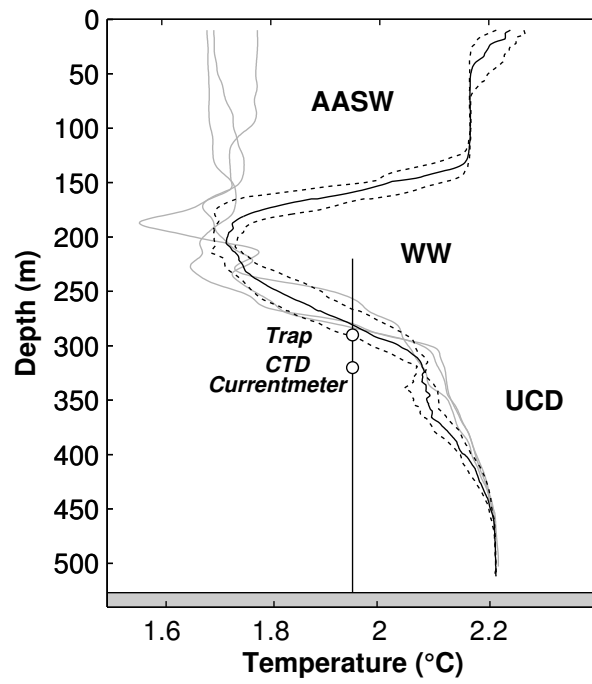
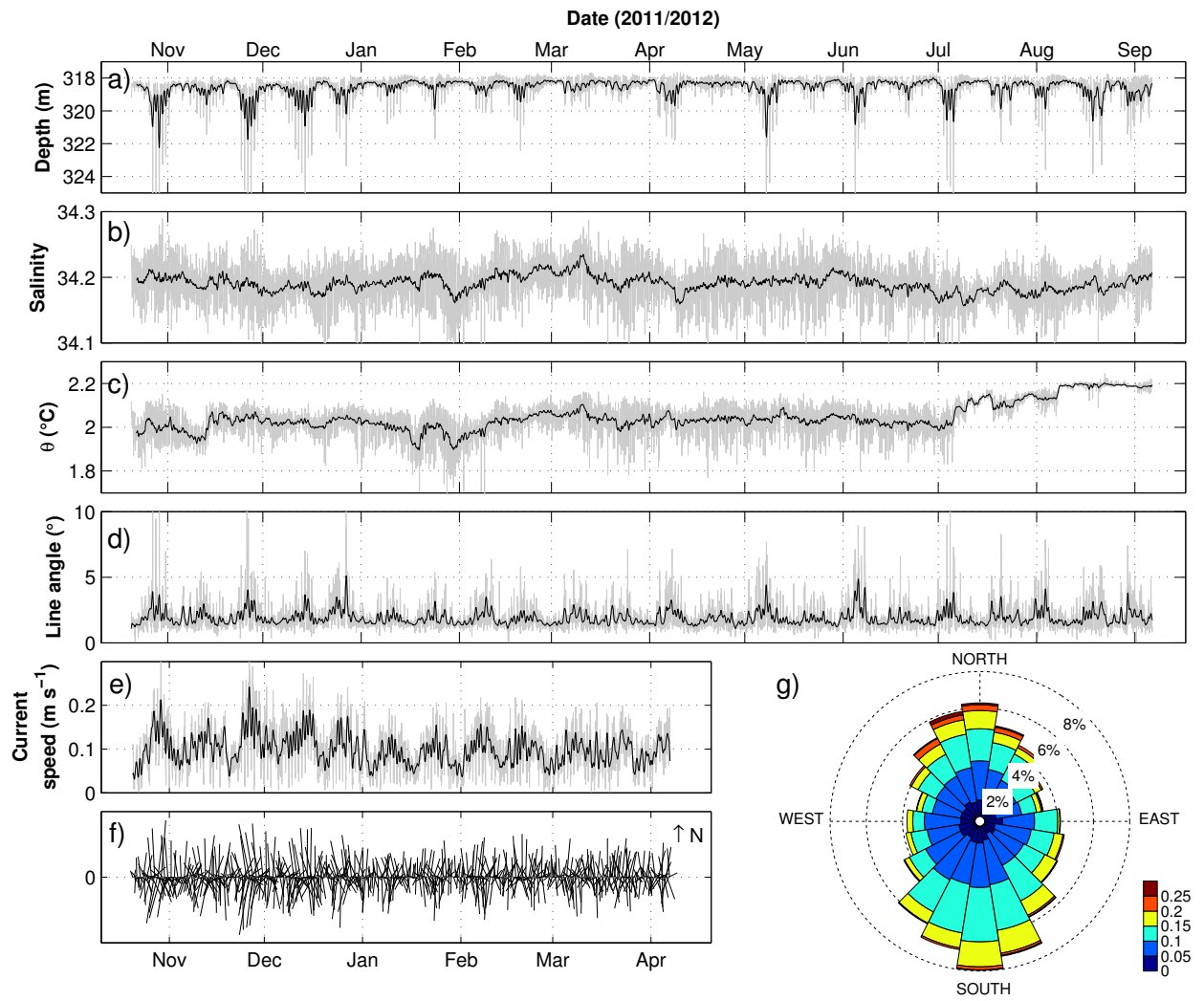


Figure 2.



**Figure 3.**

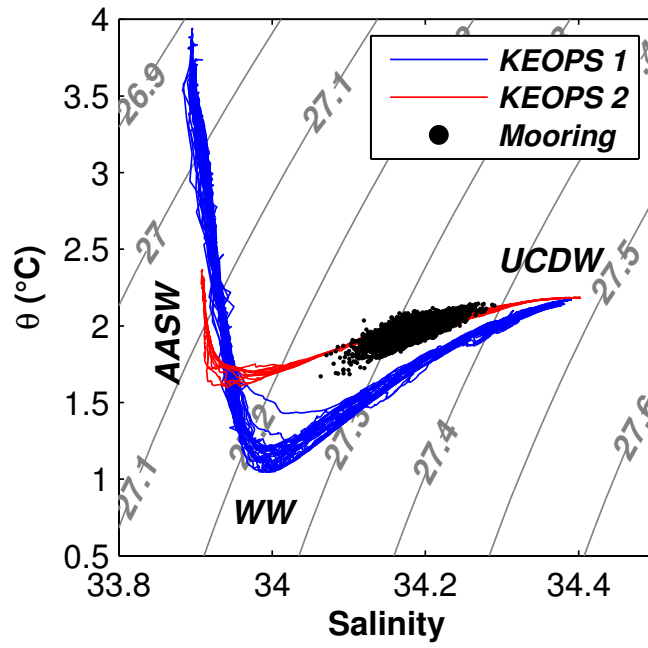


Figure 4.

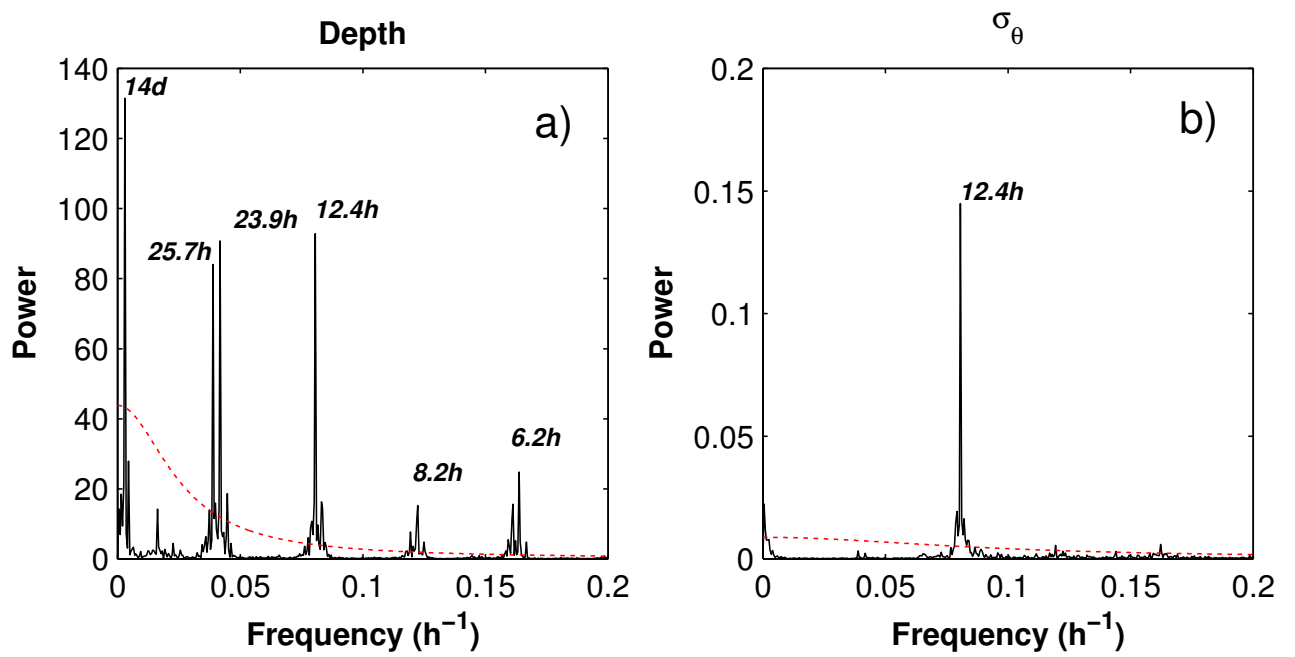


Figure 5.

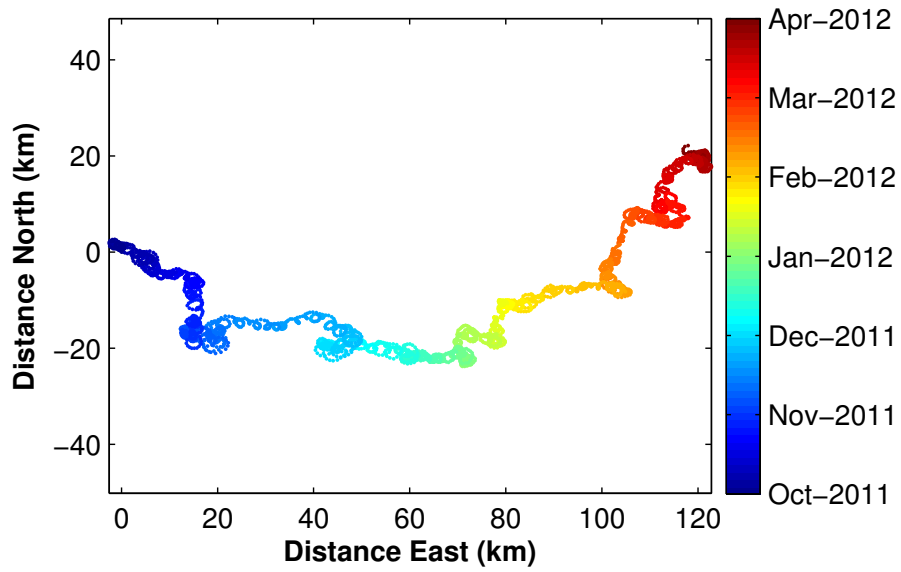


Figure 6.

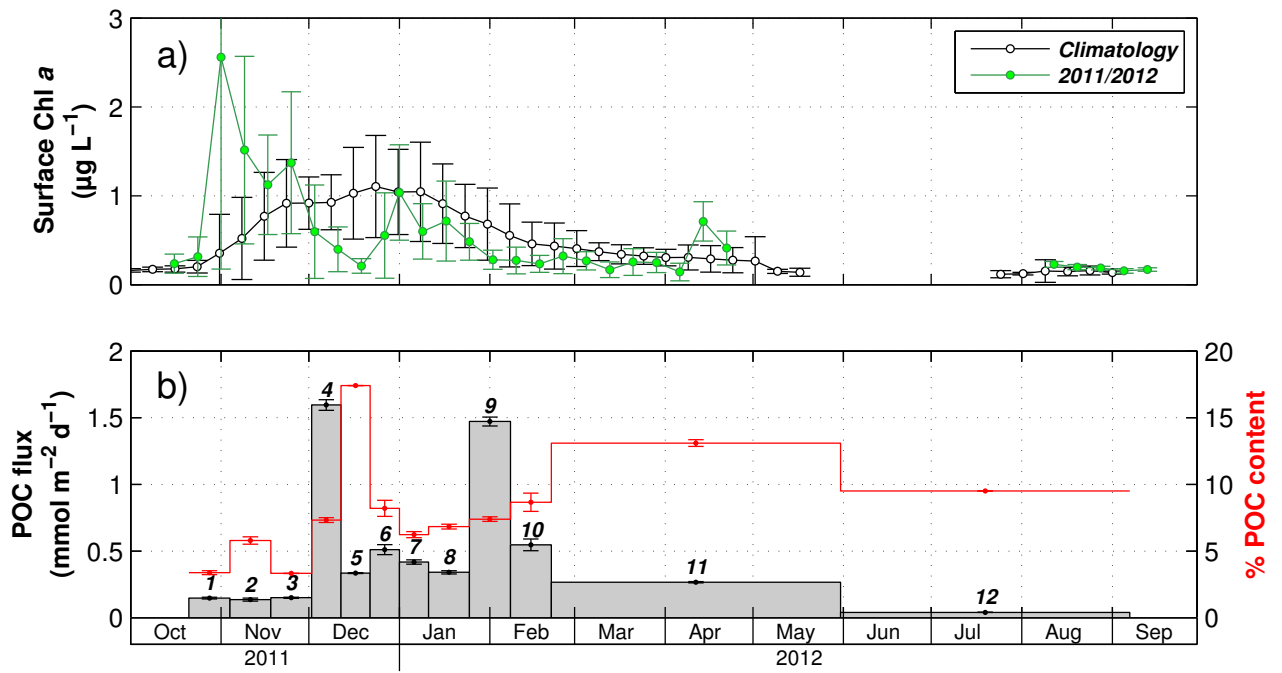


Figure 7.